https://doi.org/10.1016/j.jechem.2023.04.006

Toward stable and highly reversible zinc anodes for aqueous batteries via electrolyte engineering

Ang Li[a], Jiayi Li[a], Yurong He[b], Maochun Wu[a,*]

[a] *Department of Mechanical Engineering, The Hong Kong Polytechnic University, Hong Kong SAR 999077, PR China*

[b] *School of Energy Science and Engineering, Harbin Institute of Technology, Harbin 150001, Heilongjiang, PR China*

* Corresponding author.

E-mail address: maochun.wu@polyu.edu.hk (M. Wu).

Abstract

Featuring low cost, high abundance, low electrochemical potential, and large specific capacity, zinc (Zn) metal holds great potential as an anode material for next-generation rechargeable aqueous batteries. However, the poor reversibility resulting from dendrite formation and side reactions poses a major obstacle for its practical application. Electrolyte, which is regarded as the "blood" of batteries, has a direct impact on reaction kinetics, mass transport, and side reactions and thus plays a key role in determining the electrochemical performance of Zn electrodes. Therefore, considerable efforts have been devoted to modulating the electrolytes to improve the performance of Zn electrodes. Although significant progress has been made, achieving stable and highly reversible Zn electrodes remains a critical challenge. This review aims to provide a systematic summary and discussion on electrolyte strategies for high-performance aqueous Zn batteries. The (electro)-chemical behavior and fundamental challenges of

Zn electrodes in aqueous electrolytes are first discussed. Electrolyte modulation strategies developed to address these issues are then classified and elaborated according to the underlying mechanisms. Finally, remaining challenges and promising future research directions on aqueous electrolyte engineering are highlighted. This review offers insights into the design of highly efficient electrolytes for new generation of rechargeable Zn batteries.

Keywords: Rechargeable aqueous zinc batteries; zinc anode; dendrite growth; side reactions; electrolyte engineering.

1. Introduction

Replacing fossil fuels with renewable energies such as wind and solar is essential to achieve carbon neutrality [1-3]. However, the inherent intermittency of these renewables presents a significant challenge to their wide penetration into the energy sector, particularly the electrical grid. Large-scale energy storage systems are widely regarded as an effective solution to this challenge [4-7]. Among potential technologies, rechargeable batteries represent one of the most promising candidates because of their site-independency, high design flexibility, and high efficiency [4, 8-10]. Currently, lithium-ion batteries (LIBs) have dominated the market of electrochemical energy storage, with wide applications ranging from portable devices to electric vehicles, due to their high energy density, high efficiency, and long cycle life [11, 12]. However, the high cost, serious safety concern, and limited lithium resources severely hinder their application in grid storage [5, 13-16]. Therefore, it is imperative to develop alternative batteries that are safe and made of low-cost, abundant materials [17-23].

Among different "post-lithium-ion" batteries, rechargeable aqueous Zn batteries have attracted enormous attention because Zn metal displays a low redox potential (-0.76 V vs. standard hydrogen electrode (SHE)), high theoretical specific capacity (820 mAh g^{-1} and 5854 mAh cm^{-3}), abundant natural resources, low cost (~2-3 USD kg^{-1}), and environmental friendliness [24-28]. Moreover, the use of water-based electrolytes not only eliminates the safety issues but also endows a high ionic conductivity, which is essential to achieve high-rate capability. Additionally, the batteries can be directly manufactured under ambient conditions, offering great potential for mass production [29-32]. In fact, Zn-based batteries have been evolving over the past two centuries since the invention of voltaic cells in 1799 [33]. During this period, a wide variety of Zn batteries, including Zn-C dry batteries, alkaline Zn-MnO_2 batteries, Zn-air batteries, and Zn-Ag batteries, have been developed [34-36]. In fact, most of these alkaline batteries have been successfully commercialized and are still widely used today but only as primary power sources. Although tremendous efforts have been devoted to the exploration of rechargeable Zn-based batteries [37, 38], they have not yet become practical because of the insurmountable challenges of Zn electrodes in alkaline electrolytes. It has been demonstrated by Yamamoto and coworkers [39] in 1986 that the issues facing Zn anodes can be greatly alleviated by replacing the alkaline electrolytes with a mildly acidic electrolyte. A few decades later, Kang's group [40] discovered that Zn^{2+} ions could reversibly intercalate and de-intercalate into/from the MnO_2 cathode according to the reaction $Zn^{2+} + 2e^- + MnO_2 \leftrightarrow ZnMnO_2$. Based on this discovery, the same group [25] formally proposed the concept of "zinc ion battery" two

years later in 2011. This type of battery exhibits good reversibility, opening up great opportunities for the development of rechargeable aqueous Zn batteries (RAZBs). Since then, the research of Zn-based batteries has witnessed a boom over the past decade. To date, a wide variety of cathodes, including manganese-based oxides, vanadium-based oxides, polyanionic compounds, and Prussian Blue analogues, have been developed to pair with Zn anodes, showing great prospects for practical applications [41].

Unfortunately, all of these batteries still face challenges from Zn electrodes, although the issues are alleviated compared to those in conventional alkaline electrolytes [27, 42-45]. First, during the charging process, Zn tends to form dendrites, which not only result in low Coulombic efficiencies (CEs) and fast capacity decay, but also pose risks of short circuits. Second, due to the low redox potential of Zn^{2+}/Zn, side reactions such as hydrogen evolution reaction (HER) and direct reaction with electrolytes will take place, leading to low CEs and rapid capacity decay. Even worse, the by-products are insulated and will passivate the electrode surface, causing uneven current distribution and exacerbating dendrite growth, which in turn accelerate side reactions and battery failure. These intervened issues severely impede the practical application of Zn electrodes. To tackle these challenges, various strategies have been developed, such as electrode surface and structural modifications [46-61], separator modifications [62-65], and electrolyte engineering [66-74]. In particular, electrolyte engineering has been regarded as one of the most facile, straightforward, and effective approaches as electrolyte is a key component that largely determines the electrochemical behavior of Zn electrodes. The composition and concentration of

electrolytes directly impact the ion transport characteristics, solvated environment of Zn^{2+} ions, electrode/electrolyte interfacial properties, and (electro)-chemical stability, thereby playing a decisive role in the reversibility of Zn plating and stripping. Therefore, considerable efforts have been made to develop advanced electrolytes capable of suppressing dendrite growth and side reactions. Generally, electrolyte engineering strategies can be classified into modification of Zn salts, introduction of electrolyte additives, and employing quasi-solid electrolytes, as illustrated in Fig. 1. In this review, we summarize and systematically elaborate the recent progress in the development of high-performance mild electrolytes for Zn electrodes. We also highlight the remaining fundamental challenges and provide a prospective outlook on electrolyte engineering for achieving stable and highly reversible Zn anodes.

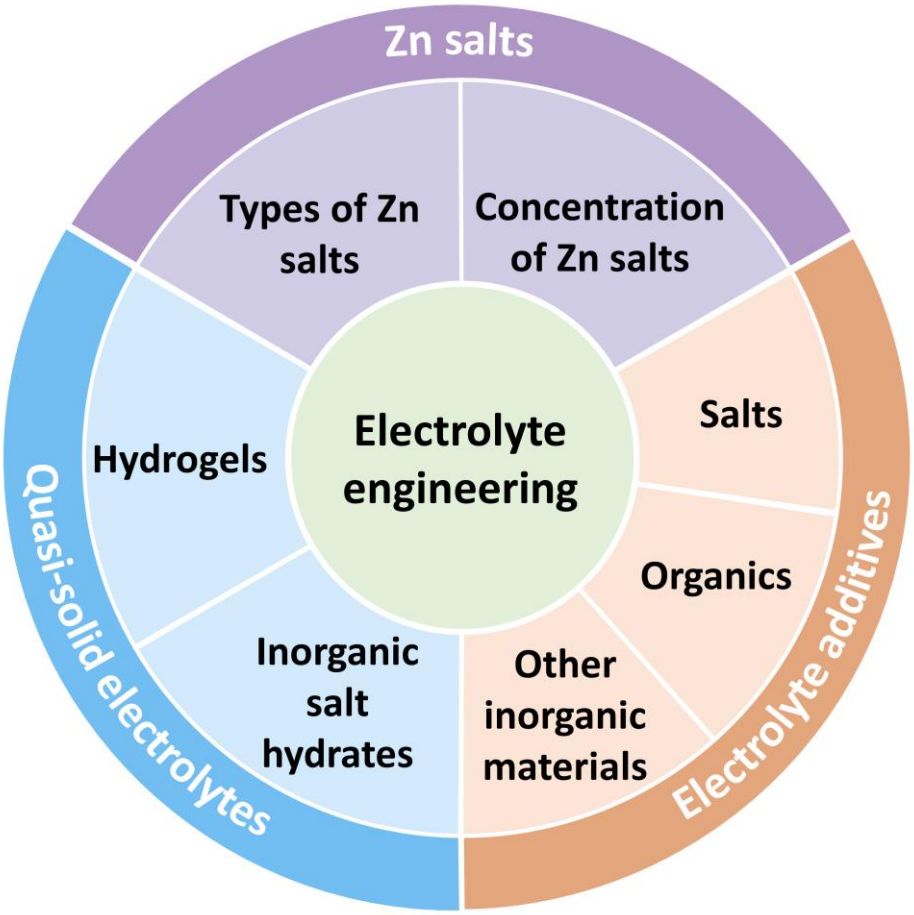

Fig. 1. Overview of electrolyte engineering strategies for achieving stable and highly reversible Zn anodes.

2. Zn electrodes in aqueous electrolytes

2.1 Fundamental electrochemistry

The overall electrochemical reaction of Zn electrode in mildly acidic solutions is shown in Eq. (1).

$$Zn^{2+} + 2e^- \leftrightarrow Zn \; E^0 = -0.76 \text{ V vs. SHE} \quad (1)$$

When the battery is being charged, Zn^{2+} ions are reduced and plated on the negative electrode while stripping of Zn takes place during the discharge process. It is

widely accepted that the Zn plating process can be divided into four basic steps as illustrated in Fig. 2. First, the solvated Zn^{2+} ions transfer from the bulk electrolyte under the applied electric field. Next, de-solvation occurs at the inner Helmholtz layer (IHL) of the electric double layer, i.e., the solvent molecules are removed from the solvation sheaths and Zn^{2+} becomes bare ions. Then, electrons are transferred from electrode to Zn^{2+} ions, forming Zn nuclei. Subsequent Zn^{2+} reduction continues to take place on the nucleation sites and Zn electrodeposits are eventually formed [75, 76]. It should be noted that all these processes will have effects on the final electrodeposit morphologies, which largely determine the reversibility of Zn electrodes. Ideally, the Zn electrodeposits should be in a dense, flat form and can be reversibly plated and stripped. However, the actual deposited Zn is usually non-uniform and dendritic, which is detrimental to the cyclability of Zn electrodes. Moreover, side reactions may occur during the electrodeposition of Zn, posing significant challenges to the development of high-performance Zn batteries.

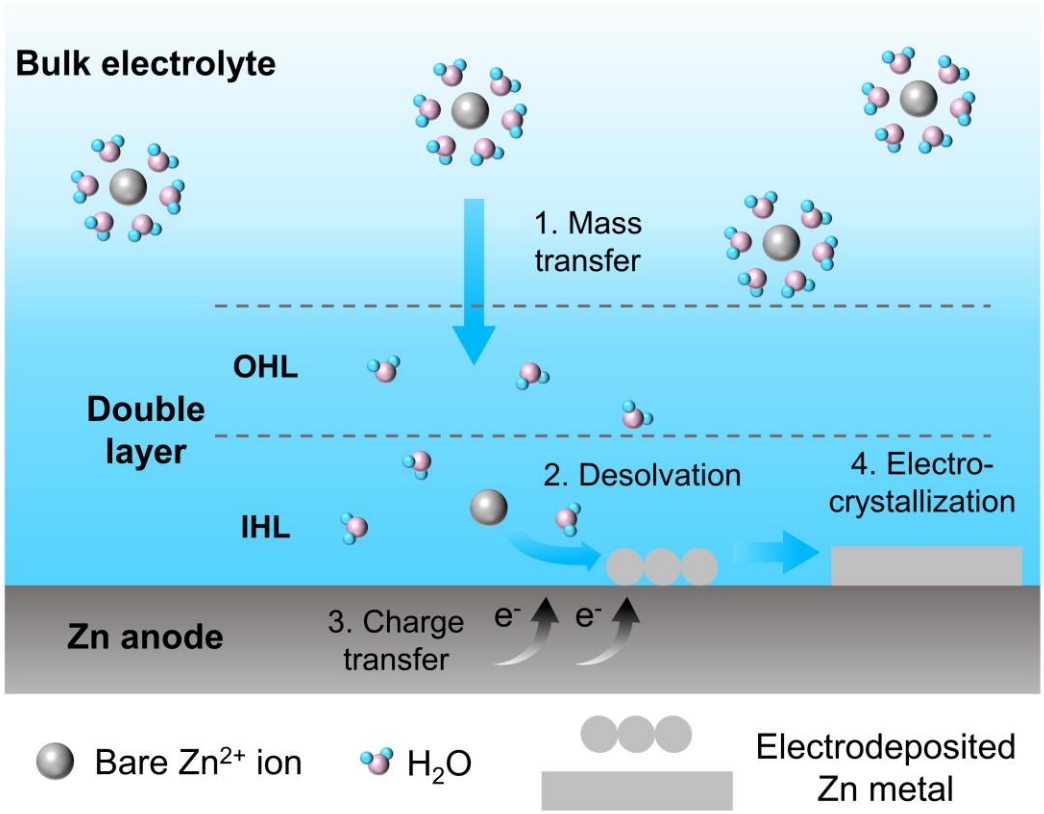

Fig. 2. Schematic of electrodeposition process of Zn^{2+} in aqueous electrolytes. (OHL: outer Helmholtz plane and IHL: inner Helmholtz plane)

2.2 Challenges of Zn anodes

Although the reversibility of Zn electrodes is greatly improved in mildly acidic solutions compared to that in alkaline electrolytes, dendrite growth and side reactions remain two major critical challenges, as depicted in Fig. 3. In this section, the root causes for these challenges are analyzed and the intrinsic connections among these problems are emphasized, which are essential for formulating solutions to boost the performance of Zn electrodes.

2.2.1 Dendrite growth

Ideally, a uniform electric field may exist if the anode surface is absolutely smooth and flat without any protrusions, which may induce uniform Zn electrodeposition. However, roughness is inevitable on actual electrode surface due to the limitation of surface finish. These protrusions exhibit a high curvature that results in a stronger local electric field and thus accumulation of Zn^{2+} ions [77, 78]. As a result, Zn will preferably deposit on these tips, known as the "tip effect" [79]. The preferential deposition will accelerate consumption of Zn^{2+} ions near the protrusions, initiating lateral diffusion of Zn^{2+} along the electrode plane for replenishment, which further attenuates the slow deposition at other locations [80]. The resulting new protrusions will further trigger non-uniform Zn deposition, causing severe Zn dendrites [81]. Furthermore, the dendritic electrodeposits are usually loosely attached to the electrode surface, and may easily detach from the electrode upon stripping to form "dead Zn", resulting in low CEs and rapid capacity decay. In addition, some remaining Zn will become nucleation sites for the following Zn deposition process, further triggering uneven Zn deposition. The accumulated Zn dendrites will grow perpendicular to the electrode, and eventually pierce the separator, resulting in internal short circuits.

In addition to the qualitative description of dendrite formation, several models have been proposed to predict the dendrite formation time. At present, the most widely used one is the Sand's time (τ_s) [76, 82], which is calculated by

$$\tau_s = \pi D \left(\frac{C_0 e z_c}{2J}\right)^2 \left(\frac{\mu_a + \mu_c}{\mu_a}\right)^2 \quad (2)$$

where μ_c and μ_a are cationic and anionic mobilities, respectively; D is the ambipolar

diffusion coefficient expressed by $D = \frac{\mu_a D_c + \mu_c D_a}{\mu_a + \mu_c}$, in which D_c and D_a are cationic and anionic diffusion coefficients; C_0 is the initial Zn^{2+} concentration; e is the electronic charge; z_c is the cationic charge number which equals to 2 for Zn^{2+}; and J is effective current density.

Based on the Sand's model, when the Zn^{2+} ions on the electrode surface are depleted at τ_s during electrodeposition process, dendrite begins to form and grow. Delaying τ_s can effectively suppress dendrite growth. From Eq. (2), it can be seen that τ_s is mainly determined by electrolyte properties and electrical conditions. Therefore, electrolyte engineering offers a promising solution to address the dendrite issue. For example, adopting a relatively concentrated electrolyte directly increases the C_0, which leads to the increase τ_s and the migration of ions (μ_c and μ_a) can be regulated by tuning the electrolyte composition and concentration. Modulating electrolytes can also alter the anode-electrolyte interface, which impacts the ion flux and effective current density and thus τ_s. Detailed discussion of these strategies is provided in section 3.

2.2.2 Side reactions

Because the redox potential of Zn^{2+}/Zn is lower than that of standard hydrogen electrode, Zn metal is thermodynamically unstable in aqueous solutions. As a result, side reactions such as HER and corrosion reactions will occur simultaneously during the Zn plating/stripping processes. Even worse, the plated Zn can directly react with electrolytes when the batteries are not in operation. The basic side reactions can be summarized in Eqs. (3)-(7).

$$2H^+ + 2e^- \rightarrow H_2\uparrow \quad (3)$$

$$2H_2O + 2e^- \rightarrow H_2\uparrow + 2OH^- \quad (4)$$

$$Zn^{2+} + 2OH^- \rightarrow ZnO + H_2O \quad (5)$$

$$Zn + 2H_2O \rightarrow Zn(OH)_2 + H_2\uparrow \quad (6)$$

$$3Zn^{2+} + 6OH^- + ZnSO_4 + xH_2O \rightarrow Zn_4(OH)_6SO_4 \cdot xH_2O \quad (7)$$

Reactions 3, 4, and 6 depict the HER, which can be chemical and electrochemical reactions that generate H_2 gas. HER side reactions are detrimental to the batteries. First, HER will consume electrolytes and lead to the formation of insulated $Zn(OH)_2$ and ZnO by-products, which will passivate the electrode surface. Second, the hydrogen bubbles absorbed on the electrode surface will block the Zn nucleation and growth sites, triggering non-uniform Zn deposition and dendrite growth. Third, for hermetic static batteries, the generation and accumulation of H_2 gas will build up the internal pressure of the batteries, leading to a serious safety concern.

In addition to HER, Zn corrosion, which can take place chemically or electrochemically, represents another major side reaction that limits the reversibility of Zn electrodes. Chemical corrosion, or self-corrosion, refers to the direct chemical reaction between Zn and electrolytes. The composition of electrolytes imposes a significant impact on the formation of by-products, as the anions are usually involved in the reactions. Take the typical $ZnSO_4$ electrolyte as an example [83]. During the dissolution process, Zn is oxidized to Zn^{2+} and dissolves in the electrolyte. The electrostatic effect drives the negative ions close to Zn^{2+}, leading to the precipitation of $Zn_4(OH)_6SO_4 \cdot xH_2O$ (ZHS), as depicted in Eq. (7), due to the very low solubility and rapid saturation. Furthermore, some anions (such as ClO_4^- and CH_3COO^- (OAc^-)) may

be preferentially oxidized or reduced before precipitation. Corrosion products in various electrolytes are summarized in Table 1. These side reactions consume electrolytes and form non-conductive substances on the Zn electrode surface, blocking the surface area available for electrochemical reactions, which is known as "passivation". It should be noted that the passivated layers are typically not uniform or dense. As a consequence, they cannot effectively terminate the side reactions. Moreover, the unevenly passivated layer will result in non-uniform distribution of current densities, thereby triggering severe Zn dendrites. In addition, due to the co-existence of different metals (i.e., Zn and current collector (e.g., Cu)) in an electrolyte, galvanic corrosion may occur, which rapidly degrades the calendar life of the batteries [84-86]. Notably, both HER and corrosion typically take place simultaneously, making it extremely challenging to distinguish the contribution of each other.

Table 1 The corrosion products in various electrolytes

Zn salt in the electrolyte	Corrosion products	Ref.
$ZnSO_4$	$Zn_4(OH)_6SO_4 \cdot xH_2O$	[87, 88]
$Zn(CF_3SO_3)_2$	$ZnO/Zn(OH)_2$, $Zn_x(OTF^-)_y(OH)_{2x-y} \cdot nH_2O$	[89, 90]
$Zn(OAc)_2$	$Zn_5(OH)_6(CO_3)_2$	[87]
$ZnCl_2$	$ZnO/Zn(OH)_2$	[73]
$Zn(NO_3)_2$	$Zn_5(OH)_8(NO_3)_2 \cdot 2H_2O$	[89]
$Zn(ClO_4)_2$	$Zn_4ClO_4(OH)_7$, $Zn_5(OH)_8Cl_2$	[91]

It is worth noting that dendrite growth and side reactions are intertwined in nature

[26, 92]. Specifically, the formation of dendrites will promote the occurrence of HER and corrosion as a result of increased surface area, which further exacerbates the side reactions [77, 79]. In turn, the by-products covered on the electrode surface will result in non-uniform distribution of current densities, further provoking dendrite growth [27, 93]. On the one hand, this is a vicious circle process because once one of the two problems occurs, if there is no timely and effective suppression, the harm will quickly expand and eventually threaten the normal operation of the battery. On the other hand, as the "positive feedback", if one issue is successfully suppressed, the other issue will be simultaneously mitigated. Fortunately, both issues are strongly linked to the electrolyte so that it is possible to simultaneously suppress dendrite growth and side reactions via electrolyte engineering, which are discussed in detail as follows.

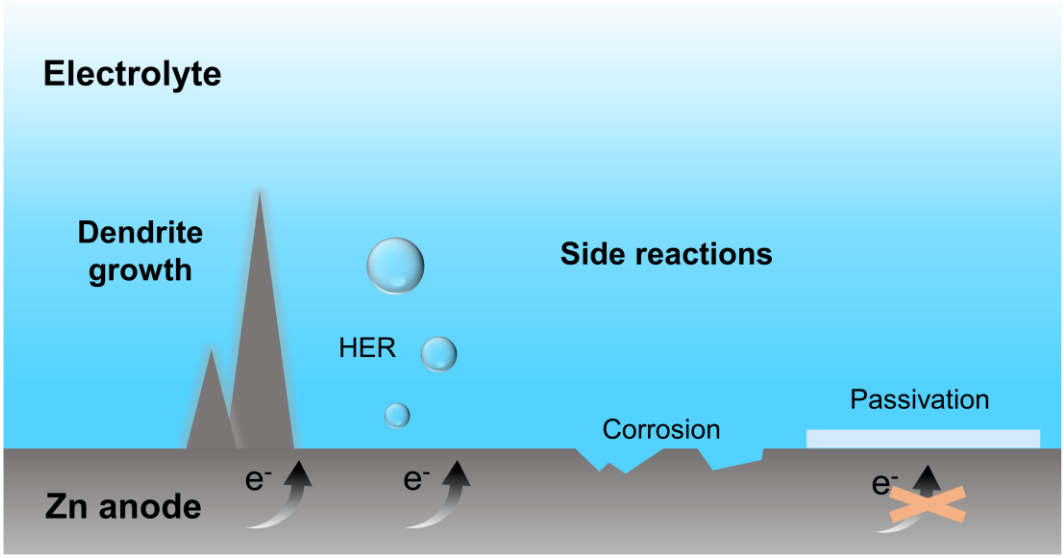

Fig. 3. Schematic illustration of the challenges faced by Zn anodes in aqueous electrolytes.

3. Electrolyte engineering for RAZBs

Electrolyte is a medium conducting ion between negative and positive electrodes, rendering it an essential component for the normal operation of batteries. More importantly, from the above discussion, it can be deduced that the electrolyte plays a critical role in determining the electrochemical behavior of Zn electrodes as it involves many of the fundamental processes. Ideally, an electrolyte should not only allow for rapid ion transfer but also prevent the occurrence of dendrite growth and side reactions, thereby leading to stable and reversible Zn plating/stripping. To this end, various electrolyte modulation strategies have been developed, which are summarized and discussed in the following sections.

3.1 Zn salts

3.1.1 Types of Zn salts

Typically, the electrolyte is prepared by dissolving a certain amount of Zn salts in a water solvent. As the anions may have a strong interaction with the Zn^{2+} ions and impact other electrolyte properties, the selection of Zn salt will have a significant effect on the electrochemical performance of Zn electrodes. $ZnSO_4$ was the first reported and most widely used Zn salt for neutral RAZBs, primarily due to its excellent features, including low cost, non-toxicity, high stability, and good compatibility with cathode materials [25, 39, 40, 94]. However, it is found that Zn electrodes in $ZnSO_4$ electrolytes usually suffer from dendrite formation and side reactions. Experimental results have revealed that the SO_4^{2-} anions take part in the corrosion process, forming an undesired

ZHS product that deteriorates the Zn electrode performance. To overcome this challenge, various salts, including zinc trifluoromethanesulfonate ($Zn(OTf)_2$), zinc bis-(trifluoromethylsulfonyl)imide ($Zn(TFSI)_2$), zinc acetate ($Zn(OAc)_2$), $ZnCl_2$, $Zn(NO_3)_2$, $Zn(ClO_4)_2$ and others, have been investigated as alternatives to $ZnSO_4$ for RAZBs. For instance, Zhang et al. [95] reported an aqueous $Zn(OTf)_2$ electrolyte for RAZBs, in which the OTf^- anion partially replaces the H_2O in the solvation sheath of Zn^{2+}. It was revealed that the $Zn(OTf)_2$ electrolyte improves the reaction kinetics and reversibility of Zn plating/stripping in comparison to $ZnSO_4$. Moreover, $Zn(OTf)_2$ can contribute to the formation of ZnF_2-containing solid-electrolyte interphase (SEI), which regulates uniform Zn deposition and suppresses side reactions by preventing the direct contact of Zn and electrolytes. Another fluorinated organic zinc salt, $Zn(TFSI)_2$, has also attracted great research interest for preparing aqueous electrolytes. The steric effects caused by the large molecular size of $TFSI^-$ and its strong interaction with Zn^{2+} can result in fewer water molecules around Zn^{2+}. Therefore, $Zn(TFSI)_2$ weakens the solvation effect and reduces the voltage hysteresis during Zn plating/stripping processes. However, the high price of these organic Zn salts may limit their practical applications. Therefore, low-cost organic zinc salts such as $Zn(OAc)_2$ appear more attractive. The weak organic acid anion of $Zn(OAc)_2$ can result in a lower H^+ concentration and thus a higher pH value of electrolyte due to the dual hydrolysis. Meanwhile, $Zn(OAc)_2$ features high environmental friendliness and good biodegradability, making it a promising candidate for RAZBs, especially when paired with vanadium-based cathodes that are acid-sensitive [96]. It has been demonstrated that 0.5 M $Zn(OAc)_2$ electrolyte enables a

Zn//$Na_3V_2(PO_4)_3$ full battery to retain 74% of capacity at 0.5 C even after 100 cycles [97]. Although OAc^- can maintain a stable pH value of electrolyte, this kind of electrolyte suppresses the kinetics of Zn plating/stripping due to its incomplete ionization and relatively low ionic conductivity. Moreover, alkaline zinc salt by-products, such as $Zn_5(OH)_6(CO_3)_2$, have been found in $Zn(OAc)_2$ electrolytes, which requires further investigation to unveil its role in the electrochemical behavior of Zn electrodes. Another common Zn salt, $ZnCl_2$, with high solubility (up to ~31 M) and low cost, has also been tried for RAZBs. However, electrolytes with a low $ZnCl_2$ concentration display a narrow electrochemical stability window, hindering their practical applications [98]. Nevertheless, the operating voltages can be widened when high concentrations are used [73], which will be discussed in the following section. The application of other common salts, such as $Zn(NO_3)_2$ and $Zn(ClO_4)_2$, is restricted by their oxidative anions, which will trigger side reactions that are detrimental to the battery performances [87, 89]. Most recently, novel Zn salts, including $Zn(NH_2SO_3)_2$ and zinc gluconate, have been proposed for RAZBs [99, 100]. These new electrolytes demonstrate encouraging electrochemical performances, showing potential to replace conventional $ZnSO_4$. However, much more works on the compatibility with cathode materials and the long-term stability are still needed to assess their feasibility for practical RAZBs.

3.1.2 Concentration of Zn salts

The concentration of Zn salt is another important factor affecting the stability and reversibility of Zn anodes. It directly determines the physicochemical properties such

as ionic conductivity, viscosity, stability, and pH value of the electrolytes, thus impacting the electrochemical processes of Zn electrodes. Generally, the higher salt concentration will bring a favorable effect on the anode. Compared to bare ions, the solvation Zn^{2+} has a higher nucleation barrier when being electrochemically reduced. Consequently, the number of nucleation sites on the Zn electrode surface is reduced and Zn dendrite growth becomes more rampant. On the contrary, more solute molecules in the electrolyte will decrease the coordination number of water in Zn^{2+} solvation sheath [101]. This change may not only weaken the energy barriers for Zn nucleation which is beneficial to uniform Zn deposition, but also mitigate the likelihood of hydrogen production from water decomposition. Meanwhile, the concentration of solute and solvent are in a reciprocal relationship. In other words, concentrated electrolytes will lower the concentration of water, thus reducing the equilibrium potential of H_2/H_2O [26, 102]. As a result, the increase in solute concentration suppresses the H_2O-induced side reactions. For instance, Wu et al. [103] systematically studied the influence of concentration of typical aqueous Zn-based electrolytes, including $ZnCl_2$, $ZnSO_4$, $Zn(OAc)_2$, and $Zn(OTf)_2$, on the electrochemical performance of Zn electrodes. Results showed that CEs of Zn plating/stripping increase with concentration in all the investigated electrolytes, suggesting the suppressed side reactions and higher reversibility of Zn electrodes in more concentrated electrolytes. Nevertheless, when the concentration of strong electron donor anions is excessively high, their intense coordination with Zn^{2+} may impose a negative effect on the electrode kinetics, although side reactions can be mitigated [104].

Note that the above electrolytes typically consist of 1-3 M Zn salts, which are known as “salt-in-water”. In these electrolytes, water molecules account for a vast majority. They partly coordinate with Zn^{2+} ions to form solvation sheaths, while others exist as free water. As Zn is thermodynamically unstable with water, it is necessary to reduce both the solvated and free water. One of the most promising solutions is to employ ultra-concentrated, or “water-in-salt” (WIS) electrolytes by dissolving a great amount of salt(s) in the electrolyte. The solvation structure changes drastically when the concentration of salts is high, particularly when approaching their solubility limit (Fig. 4a and b) [105]. Moreover, the amount of free water is dramatically reduced as they are almost entirely surrounded by solutes [106]. This unique WIS electrolyte was initially applied in LIBs with a great success [105], and was extended to RAZBs pioneered by Wang’s group [107]. They formulated a 20 m LiTFSI/1 m $Zn(TFSI)_2$ electrolyte, where m is molality in mol kg^{-1}, with a wide variety of unique properties for highly reversible Zn metal anodes. It is revealed by both theoretical structural and spectroscopic studies that the oxygen atoms coordinated with Zn^{2+} in the solvation sheath are all from $TFSI^-$ rather than water molecules. As a result, HER and dendrites are effectively prevented, leading to high Zn reversibility. When applied to a $Zn//LiMn_2O_4$ bi-ionic battery, a high energy density of 180 Wh kg^{-1} and satisfactory capacity retention of 80% after 4000 cycles were achieved.

Although this ultra-high concentration electrolytes made of organic salts boost the performance of RAZBs, the high cost and environmental issues hinder their practical applications. Alternatively, Zhang et al. [73] prepared a WIS electrolyte using abundant

and lost-cost $ZnCl_2$ salt. With a high concentration of 30 m, spectroscopic characterizations revealed that $[Zn(H_2O)_2Cl_4]^{2-}$ and $[ZnCl_4]^{2-}$ become the main form of solvated ions instead of $[Zn(H_2O)_6]^{2+}$. The formation of inert substances $Zn(OH)_2$ and ZnO is hindered owing to the reduced coordination number of water molecules. As a result, the side reactions were alleviated and 95.4% CE was achieved in an asymmetric battery. Afterwards, the same research group [108] used this electrolyte in a full $Zn//Ca_{0.20}V_2O_5{\cdot}0.80H_2O$ battery, showing a high energy density of 206 Wh kg^{-1} and long-term cycling stability (Fig. 4c). Alshareef et al. [109] reported a WIS electrolyte containing concentrated $Zn(ClO_4)_2$ and $NaClO_4$. Results show that ClO_4^- participates in the solvation sheath of Zn^{2+} (Fig. 4d), thus suppressing the water activity. Meanwhile, the preferential reduction of the coordinated ClO_4^- contributes to the formation of $ZnCl_2$ layer at the anode-electrolyte interface, which further improves the stability and reversibility of Zn anodes. The performances of RAZBs employing various highly concentrated electrolytes are summarized in Table S1. It can be seen that batteries with WIS electrolytes typically exhibit long cycling performances. However, it should be noted that the high salt concentration will usually sacrifice the ionic conductivity, which may impose a penalty on the rate performance of the batteries. Moreover, the CEs and cycling life of batteries with WIS are still not high enough to meet the requirement of practical applications. Therefore, much more efforts are still needed to unlock the potential of this strategy.

Noteworthily, a very recent study showed that ultralow-salt-concentration electrolytes could minimize the water-induced side reactions and thus expand the

electrochemical window of the electrolyte [110]. This is because decreasing the salt concentration in the electrolyte greatly reduces the content of hydrated ions, which are highly reactive species that contribute to the side reactions including HER and oxygen evolution reactions. Accordingly, a 0.3 M $ZnSO_4$ electrolyte displayed a wide electrochemical window of 2.6 V, which is 0.6 and 0.3 V wider than the commonly used 1 and 3 M electrolytes, respectively. As a result, the dilute electrolyte enabled the Zn//Cu asymmetric batteries to achieve a high initial CE of 90.96%. Moreover, as shown in Fig. 4d, the Zn//$Fe_4[Fe(CN)_6]_3$ full batteries with the new electrolyte were able to work with a high discharge medium voltage (about 1.8 V) and high cathode loading (6.80 mg cm^{-2}), opening new opportunities for developing low-cost and high-energy-density RAZBs. More importantly, these counterintuitive findings emphasize the need of fundamental studies to uncover the role of electrolytes play in Zn electrochemistry.

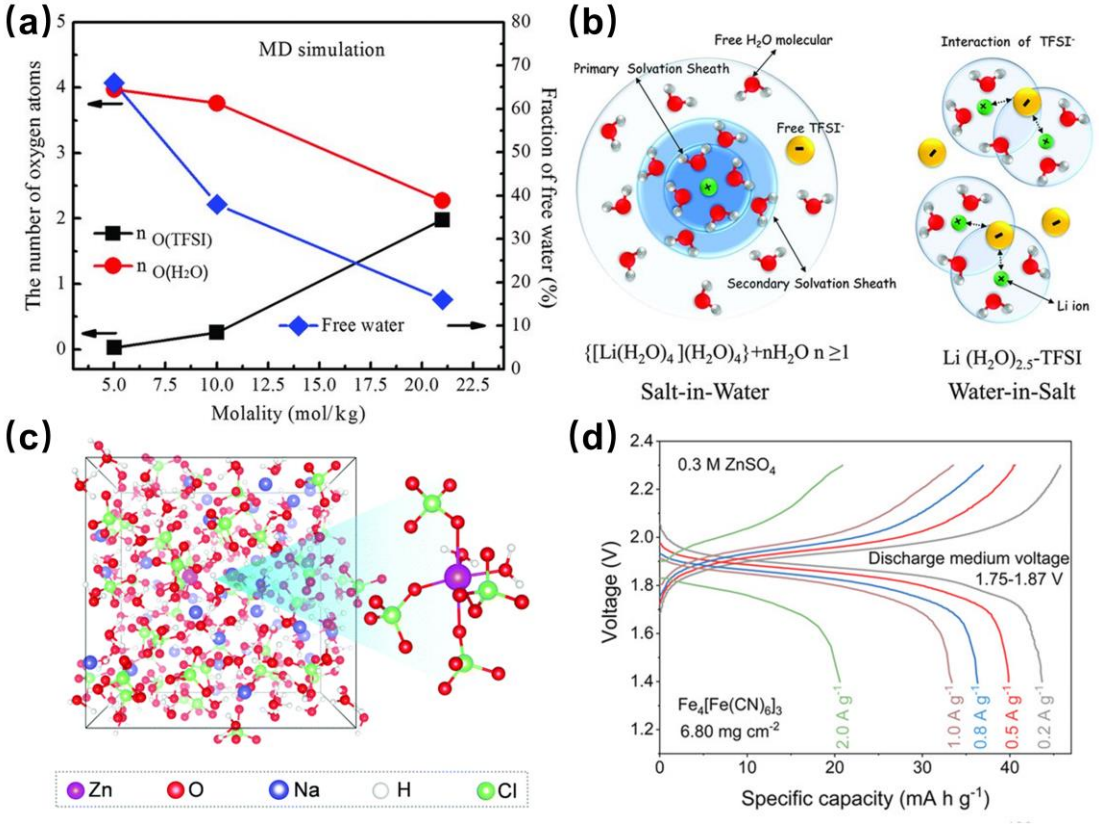

Fig. 4. (a) Numbers of water and $TFSI^-$ oxygen atoms in the Li^+ primary solvation sheath and the fraction of free water and (b) variation on the Li^+ solvation sheath in the dilute electrolyte and ultra-high concentration electrolyte. Reproduced with permission from [105]. Copyright 2015, American Association for the Advancement of Science. (c) Snapshot of molecular dynamics (MD) simulation in 0.5 m $Zn(ClO_4)_2$ + 18 m $NaClO_4$ electrolyte. Reproduced with permission from [109]. Copyright 2021, Royal Society of Chemistry. (d) Discharge and charge profiles of Zn//$Fe_4[Fe(CN)_6]_3$ full battery with 0.3 M $ZnSO_4$ at different current densities. Reproduced with permission from [110]. Copyright 2023, Wiley-VCH.

3.2 Electrolyte additives

The introduction of additives into electrolytes has proven to be a facile yet

effective approach to enhancing the performance of RAZBs. To date, a wide range of electrolyte additives have been reported, which can generally be classified into salts, organics, and other inorganic materials. The mechanisms of this approach have been gradually revealed by researchers. Some zincophilic additive molecules and electron donors may replace water molecules to coordinate with Zn^{2+}, thus forming a new solvation sheath. The additive molecules may also break the hydrogen bonding network between water molecules, thereby reducing the amount of free water and water activity in the electrolytes. In addition, some additive molecules can adsorb on the Zn anode surface or in-situ form an interfacial protective layer due to their unique valence bonds. As a result, these additives effectively regulate the Zn^{2+} deposition and inhibit dendrite formation and side reactions. In this section, electrolyte additives are discussed and elaborated based on the classifications.

3.2.1 Salt additives

Salt additives usually contain metal cations that are different from Zn^{2+}. The underlying mechanisms of this strategy depend on reduction potential of added cation compared with that of Zn^{2+} [111]. If the added cation, such as Pd^{2+} [112, 113], Ni^{2+} [113], and Bi^{3+} [114], has a higher electrode potential, its electrodeposition will occur before Zn^{2+} or co-deposition will take place, thereby regulating the subsequent Zn deposition. The other type of salt additive exhibits a reduction potential lower than Zn^{2+}. In this case, they do not undergo reduction reactions during the whole charging process. A schematic of the mechanism of these cations is illustrated in Fig. 5a. During the electroplating process, the added cations preferentially adsorb to the Zn anode surface,

especially concentrated on the tips or protrusions. Because of the aggregated positive charge, they repel the subsequent arriving positively-charged Zn^{2+} to deposit at adjacent regions, forming the so-called electrostatic shield effect. As a result, the electrodeposited Zn achieves a rather flat morphology. Thus far, various salts containing Na^{+} [115], Al^{3+} [116, 117], Ce^{3+} [66], Mn^{2+} [118], and NH_4^{+} [67, 119] have been shown to achieve the self-healing electrostatic protection [81]. Recently, new mechanisms of low-reduction-potential high-valence cationic additives have been proposed based on Derjaguin-Landau-Verwey-Overbeek (DLVO) theory by Zhao and coworkers [120]. When La^{3+} additive is introduced into the electrolyte, it competes with Zn^{2+} for adsorption on the anode surface to form the Stern layer. Each La^{3+} carries more charge than Zn^{2+} so that the total amount of ions required to neutralize the negative charge on the anode surface is reduced (Fig. 5b). In accordance with DLVO theory, the thickness of the electric double layer is reduced, which weakens the double-layer repulsion and lowers the energy barrier that needs to be overcome for the ions to approach each other, thus facilitating the Zn deposition. This phenomenon was confirmed by the calculation of Debye length and the measurement of potential. Consequently, dense electrodeposits of Zn can be achieved even at high current densities, as evidenced by the SEM images in Fig. 5c. The improved Zn deposition allows a full Zn//VS_2 battery to stably run over 1000 cycles at 1 A g^{-1} with a stable discharge capacity of about 90 mAh g^{-1}. In addition to the above two mechanisms, some additives may evolve to form a solid layer covering Zn surface. For instance, Guo et al. [121] reported that LiCl additive can suppress Zn dendrite and side reactions by forming a Li_2O/Li_2CO_3 coating layer on the Zn surface

(Fig. 5d). The performances of RAZBs using various salt additives are compared and summarized in Table S2. It can be clearly seen that the batteries with presence of salt additives display impressive performances, showing great potential in addressing key issues facing Zn electrodes.

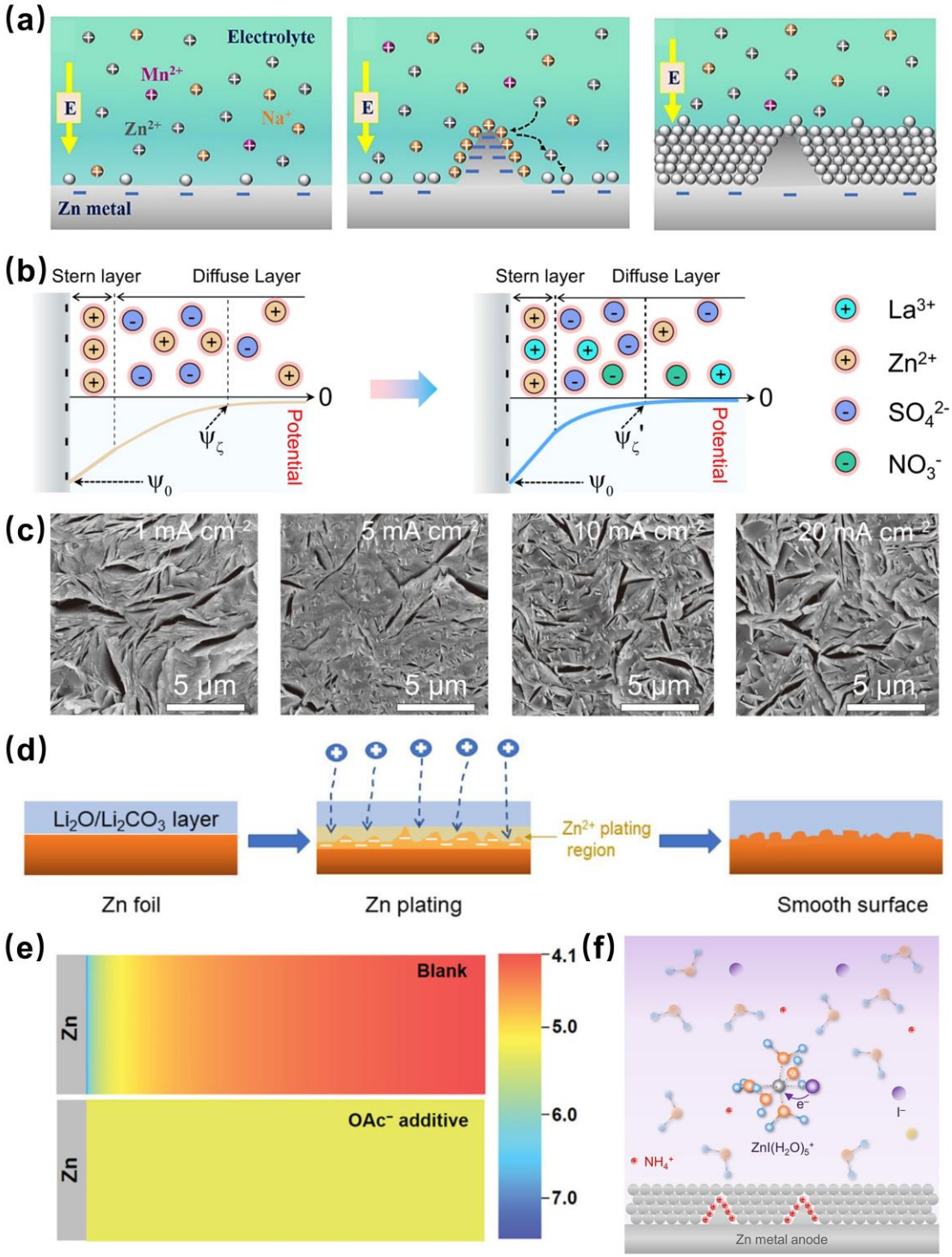

Fig. 5. (a) Schematic of electrostatic protection mechanism of Na^{+} for Zn^{2+} deposition process. Reproduced with permission from [115]. Copyright 2021, Elsevier. (b) Schematic of the comparison of the electric double layer of the Zn deposits without and with La^{3+} additive and (c) SEM images of Zn deposits in symmetric batteries with

different current densities in $La(NO_3)_3$-$ZnSO_4$ electrolyte. Reproduced with permission from [120]. Copyright 2022, Springer Nature. (d) Schematic of morphology evolution for Zn foil with LiCl added electrolyte during plating/stripping process. Reproduced with permission from [121]. Copyright 2021, American Chemical Society. (e) Simulations of the pH distribution for blank and OAc^--containing electrolytes near the Zn surface. Reproduced with permission from [67]. Copyright 2022, Wiley-VCH. (f) Schematic of stabilization of solvation structure by I^- to inhibit HER and electrostatic shielding by NH_4^+ to suppress dendrites. Reproduced with permission from [119]. Copyright 2022, American Chemical Society.

It is worthwhile noting that some salt additives will improve not only the Zn anodes but also cathodes. For example, Na^+ ions were shown to slow down the dissolution of Mn^{2+} from sodium manganese oxides in the cathode apart from suppressing Zn dendrites [115]. Moreover, the anions of the salt additives may also bring additional benefits to Zn anodes and battery performance. For instance, when NH_4OAc is used as an additive, not only can the NH_4^+ suppress the dendrite via electrostatic shield effect, but also the acetate anions can serve as a buffer in electrolyte to inhibit H^+-associated side reactions (Fig. 5e) [67]. The electron donor I^- in the NH_4I additive can involve in the solvation sheath to form $ZnI(H_2O)_5^+$ as shown in Fig. 5f, which reduces the solvated water and thus suppresses the HER [119]. The introduction Cl^- by using LiCl additive can also accelerate the Zn^{2+} transport and reduce electrode polarization [121]. These previous works indicate that when selecting salt additives, the effects of both cations

and anions should be taken into consideration at the same time to achieve synergistic effects.

3.2.2 Organic additives

Organic molecules are another popular type of additive to address the issues facing Zn anodes. So far, a rich variety of organic molecules have been proposed for RAZBs, which include liquid and solid compounds, ranging from small molecules to polymers. This section summarizes and discusses electrolyte modulation based on different organic additives. The corresponding electrochemical performances of RAZBs using different organic electrolytes are compared in Table S3.

3.2.2.1 Liquid organic molecules

Liquid organic molecules are one of the most commonly used additives for aqueous electrolytes. Extensive studies have shown that small organic molecules possess the ability to achieve stable and highly reversible Zn anodes in recent years when added into aqueous electrolytes. This function has been demonstrated for alcohols [122-129], ethers [130-132], esters [133-137], amines [138], amides [139, 140], and many other liquid organic compounds [141-146] that serve as co-solvents with water. For example, dimethyl sulfoxide (DMSO) [141, 145, 147], acetonitrile (AN) [142-144], and *N*,*N*-dimethylformamide (DMF) [139] are well known as liquid organic additives. These liquid organic additives usually possess polar groups, such as -OH, -O-, -NH_2, -COOH, -CO-, and -COO-. Consequently, they can coordinate with Zn^{2+} by replacing some water molecules to occupy solvation sheath of Zn^{2+} (Fig. 6a) [145]. The additive-regulated solvation structure can promote uniform Zn deposition, leading to reversible

Zn plating and striping. In addition, it is found that the liquid organic additives can undergo electrochemical decomposition during Zn deposition, in-situ forming an SEI that can regulate uniform deposition process and suppress side reactions. For example, Cao et al. [141] found that DMSO possesses a higher donor number than water in a $ZnCl_2$ electrolyte and thus can enter the solvation sheath of Zn^{2+}. As a consequence, fewer water molecules will coordinate with Zn^{2+}, thereby inhibiting the H_2O-induced side reactions. In addition, the solvated DMSO is decomposed to form $Zn_{12}(SO_4)_3Cl_3(OH)_{15}\cdot 5H_2O$, $ZnSO_3$, and ZnS enriched-solid SEI, which prevents the dendrite formation and side reactions. As a result, the Zn//Ti half-cells with electrolyte containing DMSO delivered a CE of 99.5% for 400 cycles and the Zn//MnO_2 full battery was able to maintain 95.3% of the initial capacity over 500 cycles. Qiao's group [148] employed γ -butyrolactone (GBL) in $ZnCl_2$ aqueous electrolyte as an additive. Spectral characterizations and theoretical calculations indicated that GBL molecules not only participate in the solvation sheath of Zn^{2+}, but also form hydrogen bonds with water molecules, thus inhibiting water-related side reactions. More importantly, a novel molecular switch mechanism was proposed. During electrodeposition, increased interfacial pH leads to ring opening of GBL to form γ-hydroxybutyrate (GHB). GHB anchors to the Zn anode surface, thereby inhibiting HER and regulating uniform Zn deposition morphology. During Zn stripping, the increase in acidity triggers the cyclization of GHB back to GBL. This dynamic modulation was proved by in-situ Fourier-transform infrared spectroscopy (FTIR). As illustrated in Fig. 6b, the intensity of characteristic absorption peaks of GBL and GHL change periodically with

plating/stripping. As a result, this strategy led to a great reversibility of Zn anode with a CE of 99.8% for Zn//Cu half-cell. Furthermore, by systematically comparing 15 organic solvent additives for regulating the EDL in aqueous electrolytes, including alcohols, esters, ethers, and sulfones, Huang et al. [149] concluded that it was the formation of SEI that contributed to the improved performance of Zn electrolytes by adding additives, rather than the donor number, adsorption energy, and dielectric constant. As the optimal additive among them, the addition of 0.5 vol% sulfolane effectively suppressed the side reactions improved the reversibility of Zn plating/striping, which can be attributed to ZnS and $ZnSO_3$-containing SEI formed in the sulfolane-added electrolyte. As a result, symmetric batteries can maintain steady cycling for over 160 h under harsh test conditions of 40 mA cm^{-2} and 10 mAh cm^{-2}.

Additionally, other fascinating features and novel mechanisms of organic fluids added electrolytes have been proposed. For instance, Wang and coworkers [122] used the high-temperature resistant and water-soluble 1,5-pentanediol (1,5-PD) as a co-solvent with water, which notably widened operating temperature range up to 100 °C for RAZBs. Zhao et al. [146] prepared a unique $Zn(OTf)_2$ electrolyte by employing *N*-methyl-2-pyrrolidone (NMP) as an additive. Similar to the principle of "end-capping" of polymerization, the NMP, which is only H-bond acceptor but not H-bond donor, cuts off the H-bonding chain. The proton transfer pathway from bulk electrolyte to interface of anode is thus interrupted and hence the HER is inhibited, leading to good cycling stability of about 1000 h for a Zn symmetric battery.

3.2.2.2 Organic chelating agents

Apart from liquid organic molecules, organic compounds with chelating ability have been explored as additives. After dissolving in the electrolytes, they will bind to the Zn^{2+} ions to form coordination complexes, thus facilitating uniform Zn deposition. So far, various chelating agents, including ethylenediaminetetraacetic acid disodium salt (EDTA-2Na) [150], 2-bis(2-hydroxyethyl)amino 2-(hydroxymethyl)-1,3-propanediol (BIS-TRIS) [151], sucrose [152], and sorbitol [153], have been reported. These previous works verify that the Zn-chelation coordination structures can alter the deposition kinetics, limit the diffusion of Zn^{2+} along the electrode surface, and reduce the active solvated water at the electrode/electrolyte interface. As a result, dendrite formation and side reactions can be simultaneously alleviated in the presence of organic chelating ligands. Additionally, the Zn-complexes can regulate the exposed crystal plane orientation to achieve uniform, dendrite-free Zn deposition. For example, thiourea (TU) can promote desolvation, selectively expose the crystalline surface for deposition, and hinder the attack of water on the anode [154]. Consequently, Zn anode with a TU-added electrolyte can be stably cycled at a cumulative capacity of as high as 3 Ah cm^{-2}.

3.2.2.3 Organic surfactants

Surfactants are a class of amphiphilic organic compounds with unique structures. Small-molecule surfactants are usually chain structures with both polar and non-polar ends. They can be classified as ionic and non-ionic surfactants depending on the chemical structure of the polar ends [155]. When added into the electrolytes, they spontaneously adsorb on the anode surface due to the strong interaction of the polar

ends with the Zn metal, while the non-polar long chains extend into the aqueous electrolytes. For example, Wang et al. [156] added oleic acid (OA) as a "temporary electrolyte additive" to the $ZnSO_4$ solution. Unlike other types of electrolyte additives that play a role in the complete life cycle of battery, this surfactant is only present in the electrolyte during the initial phase of battery operation. After the battery is assembled, OA quickly self-assembles onto the anode surface, forming an adsorption layer that can regulate uniform Zn deposition in subsequent battery operation. As a result, OA additive endows reversible Zn deposition and dissolution with an ultra-high CE of 99.63% and long life over 3340 cycles. Many surfactants, such as tetrabutylammonium sulfate (TBA_2SO_4) [157], sodium dodecyl sulfate (SDS) [158, 159], and sodium dodecyl benzene sulfonate (SDBS) [160], have also been shown to improve the performance of Zn anodes. Generally, the long hydrophobic chains of surfactants can block highly reactive water molecules to contact with Zn, thus suppressing the corrosion. Surfactants also play a positive role in reducing the surface tension of the electrolyte and increasing the wettability toward Zn metal, which is beneficial to the uniform Zn deposition. Furthermore, the molecular structure of the surfactants affects the orientation of the electrodeposits. It is well known that during plating, Zn^{2+} is deposited layer by layer parallel to the crystallographic orientation of the Zn substrate [156], and the chemisorption of surfactants is significantly selective for crystalline surfaces. Accordingly, they can lead to direction-selective Zn deposition. For instance, Lin and coworkers [161] reported sodium 3,3'-dithiodipropane sulfonate (SPS), a kind of anionic surfactant, as an additive for RAZBs. Density functional theory (DFT)

calculations revealed that SPS anions tend to adsorb on (100) and (101) facets of Zn metal instead of (002). Therefore, Zn^{2+} was constrained to deposit on the exposed (002) facet, leading to the horizontal plating pattern (Fig. 6c). The uniform deposition was further proven by flat surfaces in in-situ optical microscopy and electrochemical atomic force microscopy (AFM) images (Fig. 6d and e). More remarkably, it was demonstrated that the presence of SPS enabled a pouch-type RAZB to deliver a high areal capacity of about 2 mAh cm^{-2} and retain 82.8% of its initial capacity after 200 cycles. It was also found that SDS and SDBS favor the deposition of Zn^{2+} in the (002) and (103) directions [158], while OA leads to preferential growth of Zn (002) plane [156]. In addition, the charge structure of the polar end of the surfactants affects the diffusion and migration of Zn^{2+} ions. For instance, the cations of TBA_2SO_4 surfactant accumulate in the protuberances of anode surface, preventing the deposition of Zn^{2+} at these areas due to electrostatic repulsion [157]. Furthermore, nonionic polymer surfactants, such as polyethylene glycol (PEG) with different molecular weights [162], have also been found to promote smooth Zn deposition. Unlike the surfactants with the "head-tail" structure described above, the polar group -O- in the main chain of PEG allows parallel adsorption along the anode surface. It can alleviate the notorious dendrites by reducing the exchange current density and prohibiting the 2D diffusion of Zn^{2+}. The PEG adsorption layer on the anode surface can also slow down the HER. More attractively, when some surfactants are added to the electrolyte, they can "kill two birds with one stone". That is, they slow down the adverse reactions of the cathode and stabilize the Zn anode at the same time, thus enhancing the overall battery performance [160].

However, it should be noted that the amount of added surfactant should be meticulously determined. On the one hand, if the amount is too small, the positive effects may not be significant. On the other hand, if too much surfactant is added, the increased interfacial resistance and electrode polarization caused by the adsorption layer of surfactants may impose an adverse effect on the electrochemical performance of RAZBs.

3.2.2.4 Polymers

Polymers with large molecular weights also show promise as additives for RAZBs. Poly(ethylene oxide) (PEO) has the same chain units as PEG but a higher degree of polymerization. Therefore, PEO presents a similar modulation mechanism to that of PEG as shown in Fig. 6f [163]. The difference is that PEO with higher molecular weight has a greater effect on electrolyte viscosity, which is closely related to ion migration. It was shown that these substances possess preferential adsorption to different crystalline surfaces. Besides, some polymers are also reported to take part in the solvation sheath, especially those with relatively low molecular weight [164, 165]. For example, polyacrylamide (PAM) can preferentially adsorb on the electrode surface and induce uniform Zn^{2+} flux through the -CO-NH_2 groups, thus leading to uniform Zn deposition [166]. With the addition of PAM, a Zn symmetric battery with 80% depth of discharge (DOD) can be cycled for 350 h and Zn//MnO_2 full battery is capable of running for 600 cycles with a capacity retention of 98.5% at 1000 mA g^{-1}. Interestingly, Zhang's group [167] reported that a non-ionic polymer, polyvinylpyrrolidone (PVP), also exhibits the electrostatic shielding effect. Combined with DFT calculations, it was revealed that the nitrogen atom of PVP absorbs on the tip of Zn anode, preventing the development of

Zn protrusions and thus leading to smooth Zn plating. SEM images showed that the Zn surface remains flat with hexagonal-like flakes even after 1000 charge/discharge cycles in the PVP-containing electrolyte, confirming PVP is a highly efficient additive for RAZBs.

3.2.2.5 Natural organic compounds

In addition to the aforementioned synthetic organic compounds, natural substances are gaining more and more attention, such as amino acid molecules containing -NH_2, -COOH, and side chain groups (-R). After selection and analysis, Meng and coworkers [168] chose cysteine as an additive for RAZBs. Cysteine is the only amino acid with a -SH side chain group. Thus, it strongly interacts with Zn metal and Zn^{2+} to optimize the electrode-electrolyte interface and the solvation structure, respectively. Consequently, a stable and reversible Zn anode is obtained in the presence of cysteine additive, enabling the Zn//MnO_2 full batteries to operate for more than 700 h. Xu et al. [169] successfully utilized the $ZnSO_4$-induced secondary structure transition of silk fibroin (SF). The helical SF turned into random coils and thus exposing more -NH_2 and -COOH groups. SF was shown to effectively break the hydrogen bonding network of solvent and replace the water molecules in the solvation sheath of Zn^{2+}, thereby significantly suppressing HER. Meanwhile, as the XPS results in Fig. 6g and h show, N atoms in SF are strongly adsorbed on the Zn surface, in-situ forming a protective film to guide uniform Zn deposition. As a result, the cycle life of the symmetric Zn battery is considerably boosted, demonstrating stable charging and discharging over 1600 h.

Recently, Qiu et al. [68] reported an anion-trap additive (i.e., cyclodextrins (CDs))

for RAZBs based on the host-guest interaction chemistry. CDs are a series of cyclic oligosaccharides generated by the enzymatic action of straight-chain starch, and those with six- to eight-membered rings are most commonly known as α-, β-, and γ-CD. Since CD is hydrophilic in rim and hydrophobic in cavity, it is capable of selectively enveloping the appropriate guest by non-covalent interaction as a host. In the $Zn(ClO_4)_2$ electrolyte, both theoretical calculations and experimental characterizations confirmed the formation of β-CD@ClO_4^- complex while the other two kinds of CDs did not exhibit this property (Fig. 6i). Diffusion coefficient obtained from MD simulations (Fig. 6j) reveals that the β-CD@ClO_4^- restricts the random motion of the solute anion and enhances the cation migration number in the electrolyte. This complex also prefers to adsorb on the (002) crystal plane of Zn metal, thus guiding the formation of Zn (002) texture. Consequently, regular and uniform Zn deposition can be achieved, as indicated in Fig. 6k. As a result, Zn//Zn symmetric battery exhibits 10 times longer cycle life and Zn//MnO_2 full battery displays a 57% capacity increase in comparison to the batteries with pure $Zn(ClO_4)_2$ electrolyte. Interestingly, Ho's group [170] prepared an impact-resistant RAZB by taking advantage of the shear-thickening feature of cornstarch aqueous solution at a high concentration of 55 wt%. The natural polymer solution exhibits common fluid-like properties without external forces, which offers a satisfactory Zn^{2+} conductivity (3.9×10^{-3} S cm^{-1}) and transference number (0.251), thereby allowing the battery to operate under normal conditions. When the battery is suddenly subjected to shear stress, the electrolyte instantly becomes as rigid as a solid, enabling the battery to avoid accident-induced damage and short circuits. This unique

feature is highly required for batteries that need to operate under harsh conditions (e.g., military applications), and much more effort is needed to push the development of impact-resistant batteries.

To sum up, a wide range of organic additives have been reported to tackle the challenges of Zn anodes in aqueous electrolytes. Although the types of these additives can generally be categorized, most of them share similar mechanisms, namely coordinating with Zn^{2+} and absorbing on the electrode surface, thereby regulating Zn deposition and suppressing side reactions. Nevertheless, many novel mechanisms are being proposed and unraveled when unique organic additives are used. In fact, it can be anticipated that much more powerful additives will be developed in the future given the highly tunable structure of organic molecules, particularly with the aid of high-throughput computation and artificial intelligent. However, it should be pointed out that the compatibility with cathode and long-term stability should also be considered when selecting/designing organic additives. Fundamental studies on the degradation mechanisms of current organic additives during cycling may shed light on the development of highly durable organic molecules for RAZBs.

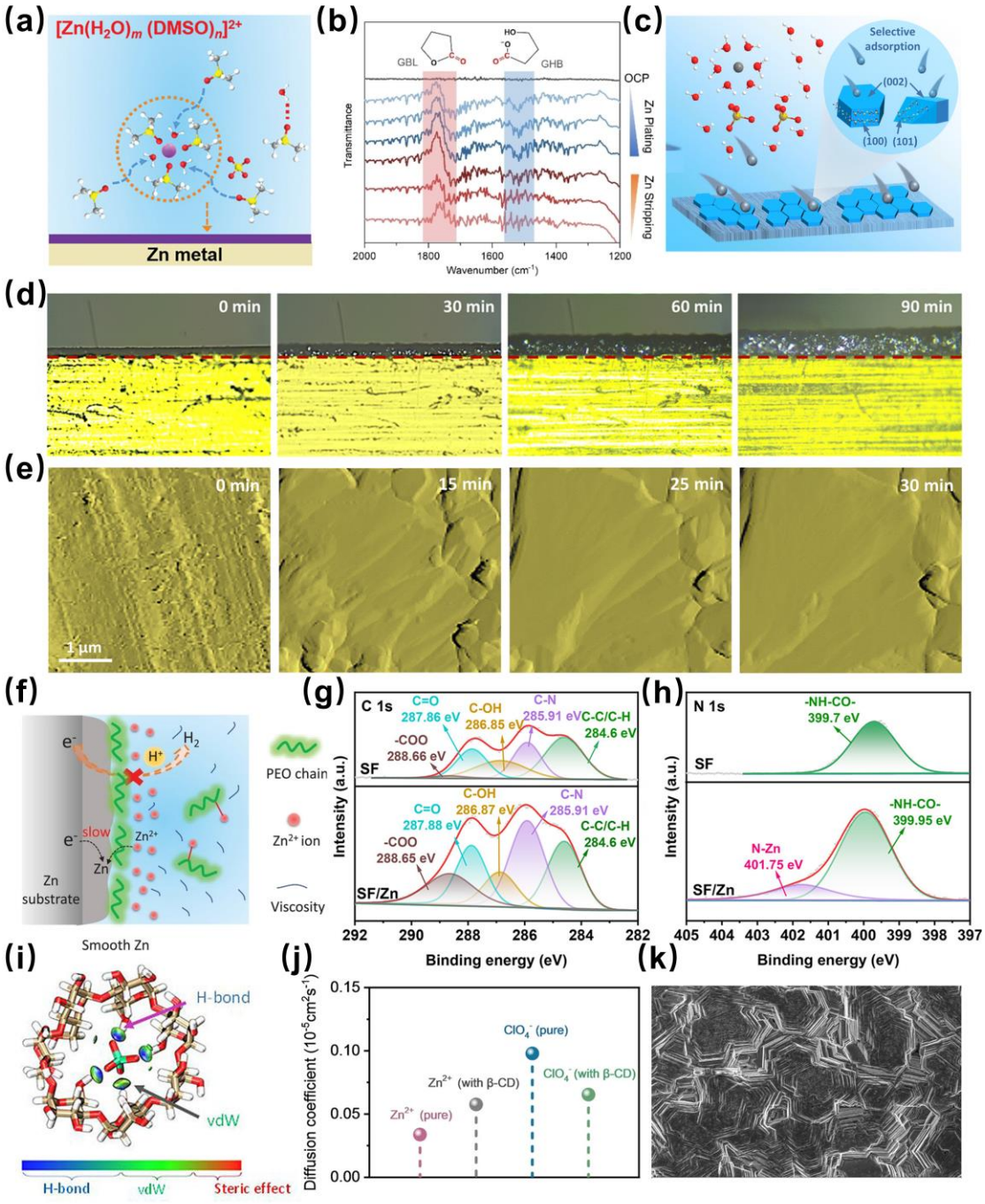

Fig. 6. (a) Schematic of the novel solvation structure of Zn^{2+} in DMSO-added electrolyte. Reproduced with permission from [145]. Copyright 2021, Wiley-VCH. (b) In-situ FTIR of the anode-electrolyte interface upon plating/stripping. Reproduced with permission from [148]. Copyright 2023, Wiley-VCH. (c) The schematic of the Zn electrodeposition process in $ZnSO_4$ electrolyte with SPS additive, (d) in-situ optical

microscope, and (e) in-situ electrochemical AFM images of the Zn electrodeposition process in SPS-added electrolyte. Reproduced with permission from [161]. Copyright 2023, Royal Society of Chemistry. (f) The schematic of PEO additive promoting smooth Zn deposition and inhibiting HER. Reproduced with permission from [163]. Copyright 2020, Wiley-VCH. (g) C 1s and (h) N 1s XPS spectra of SF and Zn foil immersed in SF solution. Reproduced with permission from [169]. Copyright 2022, American Chemical Society. (i) Independent gradient model (IGM) analysis of *β*-CD@ClO_4^- complex, (j) diffusion coefficient of Zn^{2+} and ClO_4^- in electrolytes with and without *β*-CD additive derived from MD simulations, and (k) SEM image of the Zn electrode obtained by plating at 10 mA cm^{-2} in $Zn(ClO_4)_2$ electrolyte containing *β*-CD. Reproduced with permission from [68]. Copyright 2022, Wiley-VCH.

3.2.3 Other inorganic materials additives

In recent times, nanomaterials with 2D layered planar structures, which possess high specific surface area and abundant surface functional groups, have sparked researchers' interest in using them as electrolyte additives. Sun et al. [171] pioneered the incorporation of $Ti_3C_2T_x$ MXene into the electrolyte. Theoretical calculations combined with experiments showed that the intense adhesive effect of the -O groups on the surface of etched nanosheets to Zn^{2+} firstly enables the formation of the MXene-Zn^{2+} combination. Then the zincophilic MXene easily constructs the robust SEI that facilitates highly reversible Zn plating/stripping without dendrite formation. Meanwhile, MXene nanosheets shorten the pathways for the diffusion of Zn^{2+}, which

yields faster electrode reaction kinetics (Fig. 7a). As illustrated in Fig. 7b, this first-of-its-kind approach enables the Zn symmetric battery to achieve over 1000 stable cycles. Similarly, 2D layered graphene oxide (GO) was used as an additive by Abdulla and coworkers [172]. It was demonstrated that $ZnSO_4$/GO electrolytes could be obtained simply by ultrasonic dispersion. Extensive characterizations and tests revealed that GO not only strongly interacts with Zn^{2+} but also intensely adsorbs on Zn electrodes. This unique property homogenizes the electric field distribution at the electrode/electrolyte interface, drives the movement of Zn^{2+} toward the anode, and decreases the charge transfer resistance and nucleation overpotential. Results indicated that the full battery with GO delivered a high-capacity retention of 93% after more than 250 cycles.

Moreover, palygorskite, a natural clay with microstructure between the 1D chain and 2D lamellar, was used by Gao et al. [173] to prepare high concentration of colloidal electrolytes (HCCE). As displayed in Fig. 7c, metal cations in the octahedral sheets of palygorskite will be replaced by Zn^{2+}, so that the concentration gradient-controlled ion exchange occurs in HCCE. This substitution reaction keeps Zn^{2+} from being surrounded by solvent water molecules. Collectively with palygorskite's adsorption of free water and repulsion of solvent anions, side reactions are dramatically suppressed. Moreover, HCCE exhibits a similar ionic conductivity (11 mS cm^{-1}) and higher Zn^{2+} transference number (0.64) than conventional aqueous electrolytes, which are beneficial for high-rate performance of Zn electrodes. As a consequence, the Zn//HCCE//α-MnO_2 full battery achieved an 89% capacity retention after 1000 cycles at a high current density of 0.5 A g^{-1}.

To achieve high DOD and high areal capacity, which are critical for practical applications, Zhang et al. [69] proposed and demonstrated a dynamic reversible SEI controlled by adding graphitic C_3N_4 (g-C_3N_4) nanosheets into the electrolyte. As shown in Fig. 7d, during electrodeposition, the electric field is directed vertically toward the Zn anode. The cations attracted by the electron donor on the g-C_3N_4 surface migrate in the direction of the anode, and the resulting polarization causes the nanosheets to be torqued. Eventually, the electric field force aligns them perpendicular to the Zn anode. Theoretical calculations and experimental characterizations revealed that these nanosheets with crystallographic match to Zn are preferentially adsorbed on the (0002) facet, driving ordered and compact electroplating of Zn. In the subsequent plating/stripping, the nanosheets are hardly consumed but undergo adsorption/desorption periodically. Consequently, remarkable reversibility is achieved even at a severe testing condition with an areal capacity of as high as 20 mAh cm^{-2}. The authors also claimed that this strategy could be extended to other nanosheet additives (e.g., boron nitride (BN)) and other resource-rich rechargeable metal batteries, including Mg and Al. Likewise, Li's group [70] developed C_3N_4 quantum dots (C_3N_4 QDs) as an additive for RAZBs. The zincophilic nanopores on the surface of the C_3N_4 QDs act as Zn^{2+} carriers and separate Zn^{2+} from water molecules (Fig. 7e and f), which regulates the Zn^{2+} flux and modulates the solvation structure. Coulombic forces cause the C_3N_4 QDs to build an "ion sieve" protective layer, which selectively conducts Zn^{2+} while blocking water molecules, thus allowing uniform Zn deposition. Interestingly, the protection layer enabled by C_3N_4 QDs can "self-assemble-disassemble-reconstruct"

with potential reversal during charging and discharging, demonstrating a powerful self-repairing ability to guard the stable operation of RAZBs. By introducing C_3N_4 QDs into pristine $ZnSO_4$ electrolyte, 93.5% capacity retention was achieved for a Zn//$VOPO_4$ full battery after 3000 cycles.

As mentioned earlier, ZHS is the typical by-product of $ZnSO_4$ electrolyte. Theoretically, it possesses high zincophobicity, high ionic conductivity, and low electronic conductivity. Although all of these properties are necessary for an efficient SEI, the ZHS generated during cycles has a random distribution and uneven structure, which fails to protect Zn anodes. To overcome this issue, Xin et al. [88] exquisitely designed a $Zn(OH)_2$-containing electrolyte, which turns the ZHS by-product into a uniform protective layer. The in-situ formed SEI can not only inhibit dendrite growth and side reactions, but also enhance the reaction kinetics of Zn electrode. Accordingly, both remarkable cycling performance (>1190 h under 2 mA cm^{-2} with 2 mAh cm^{-2}) and rate performance (low overpotential of 75 mV at 10 mA cm^{-2}) of the battery were achieved. The performances of Zn anodes and RAZBs with other inorganic materials additives are summarized and compared in Table S4. It is clear seen that the batteries with the presence of other inorganic materials in the electrolyte deliver impressive cycling performance, demonstrating their promise for development of durable RAZBs.

Noteworthily, the aforementioned inorganic materials usually exist as suspended solids in the electrolytes, which differ radically from conventional additives that are soluble. Hence, the mechanisms underlying Zn deposition/dissolution processes also vary [174]. Although several mechanisms have been proposed in previous works, much

more efforts are needed to unlock the great potential of this type of emerging additive, given the large family and unique properties of nanomaterials. Systematically studying the effects of morphologies, functional groups, particle sizes, and concentrations of different nanomaterial additives on the electrochemical behavior is essential to establish the composition-property-performance relationship that will inform the optimal design. In addition to Zn anode, how the addition of inorganic nanomaterials affects the separator/cathode and thus the overall electrochemical performance should be taken into consideration, as the nanomaterials may absorb onto these key components. Moreover, since nanoparticles may aggregate over time, it is essential to evaluate the long-term stability of nanofluids for RAZBs.

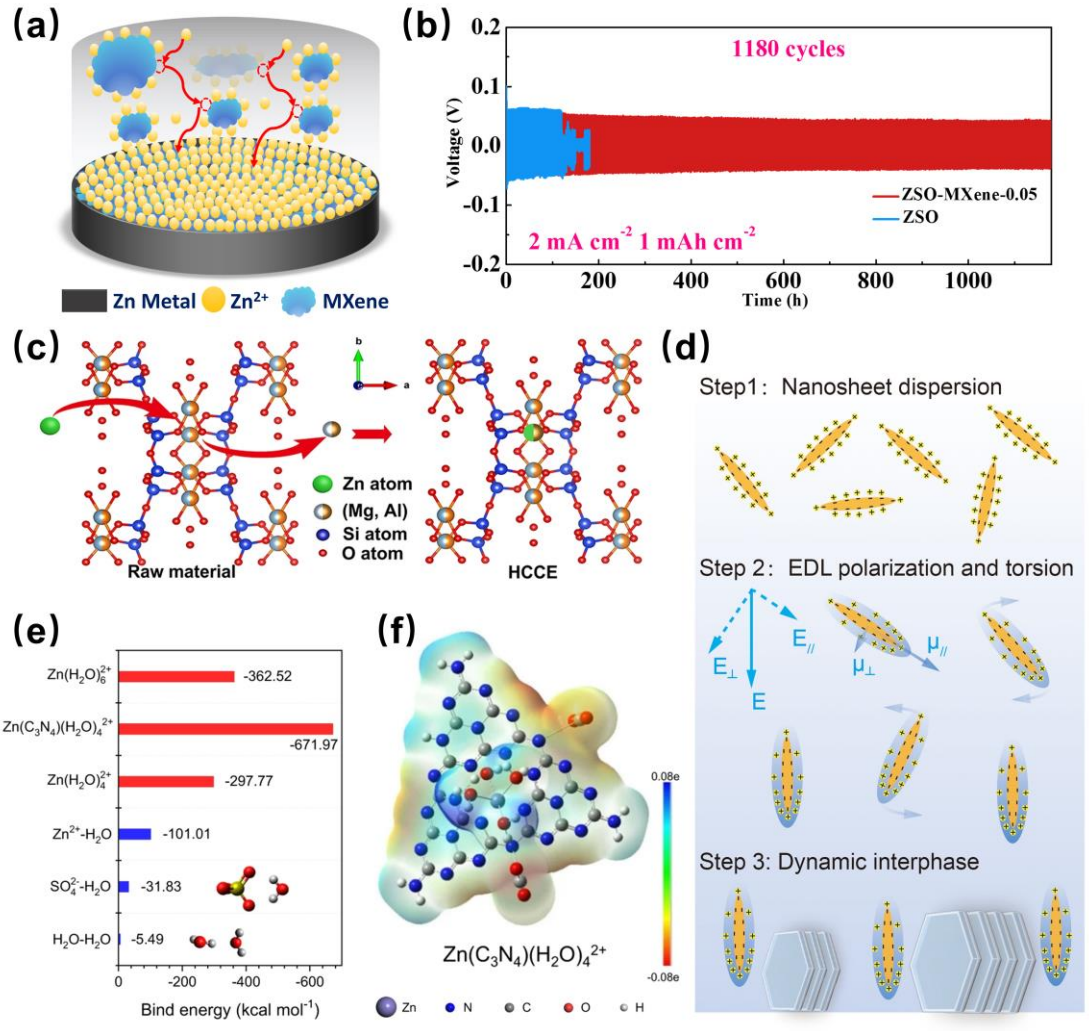

Fig. 7. (a) Schematic of the effect of MXene additive on the Zn deposition process and (b) long-term galvanostatic cycling of symmetrical batteries with and without MXene. Reproduced with permission from [171]. Copyright 2021, Springer Nature. (c) Schematic of ion exchange in the HCCE. Reproduced with permission from [173]. Copyright 2021, Springer Nature. (d) Schematic of electro-orientation process. Reproduced with permission from [69]. Copyright 2021, American Association for the Advancement of Science. (e) The binding energies of Zn^{2+} solvation configurations based on the DFT calculations and (f) the electrostatic potential distributions of $[Zn(C_3N_4)(H_2O)_4]^{2+}$ solvation structures. Reproduced with permission from [70].

3.3 Quasi-solid aqueous electrolytes

Although liquid electrolytes as discussed in the previous sections have intrinsic advantages in high ionic conductivity and ease of preparation, they have some drawbacks such as leakage. Moreover, in aqueous electrolytes, the deposition of Zn is free of external force, which is also one of the possible reasons for severe dendrite growth. These issues can potentially be addressed by employing quasi-solid aqueous electrolytes, i.e., hydrogel electrolytes and inorganic salt hydrates electrolytes.

3.3.1 Hydrogel electrolytes

In hydrogel electrolytes, water molecules are anchored within a 3D polymer network formed by cross-linking. The hydrophilic groups (such as -OH, -COOH, and -NH_2) in the macromolecular chains of hydrogel make itself solvent-rich and highly swollen. Physical and chemical cross-linking allow hydrogel to maintain a certain shape. Thus, hydrogel is a soft matter with both liquid and solid properties. In RAZBs, Zn^{2+}-containing hydrogel can take on the roles of both electrolyte and separator [92]. The adsorption of solvent by the massive number of hydrophilic groups through non-covalent interactions greatly reduces the reactivity of free water, therefore mitigating the side reactions. Moreover, the interaction between Zn^{2+} ions and the functional groups of hydrogel electrolytes can regulate the uniform flux of Zn^{2+}, thus restraining dendrite formation. In addition, unlike pure liquid electrolyte, hydrogel with certain mechanical properties can also suppress dendrite growth. Furthermore, remarkable

progress has been achieved in endowing hydrogel with smart functionalities, such as self-repairing, self-protection from thermal accumulation, and wide temperature adaptability. So far, a wide range of synthetic hydrogels, including poly(vinyl alcohol) (PVA), PAM, and poly(2-acrylamido-2-methylpropane sulfonic acid) (PAMPS), and natural hydrogels derived from biomass, such as xanthan gum, and hybrid hydrogels have been developed and employed as electrolytes in RAZBs as summarized in Table S5 [71, 175-184]. Furthermore, the flexibility of hydrogels makes it possible for RAZBs to be fabricated in various shapes and sizes, such as cable-type battery [176], yarn battery [185], and fiber-shaped battery [186], as displayed Fig. 8a-c. Because of their great flexibility, they show great promise as power sources for wearable devices. However, more efforts are needed to improve the ionic conductivity and mechanical properties, as well as optimize electrode/electrolyte interfaces, to further boost the performance of RZABs.

3.3.1.1 Properties of hydrogel electrolytes

Mechanical strength is one of the most important properties that affect the performance of hydrogel-based RAZBs. Unfortunately, conventional hydrogels with a large amount of water usually exhibit poor mechanical strength. To address this issue, high-strength quasi-solid electrolytes have been developed by applying different energy-dissipative methods such as double-network (DN) hydrogels and nanocomposite hydrogels. As shown in Fig. 8d, Liu et al. [71] prepared PAMPS with rigid macromolecular chains as the first network, which was then immersed in acrylamide solution to trigger the second polymerization step, which improves the

flexibility of PAM network. The tensile strength of PAMPS/PAM DN hydrogel is almost three times higher than that of the PAM hydrogel. In addition, the nanocomposite hydrogel prepared by Mo et al. [187] using cellulose nanofibrils as reinforcing phases also possesses strong tensile properties. The -OH and -COOH groups in cellulose form an H-bond-dominated interphase with a gel matrix for effective load transfer. Consequently, this reinforced hydrogel electrolyte presents a tensile modulus of up to 24.46 kPa and a strain of 920%, whereas the pristine hydrogel only exhibits a tensile modulus of 6.55 kPa. The excellent mechanical properties of the as-developed hydrogel enable the batteries to operate normally even when bent through 180°.

Ionic conductivity is another significant factor that determines the rate capability and power density of RAZBs. Due to the 3D-polymer network structure and inevitable water evaporation, ionic conductivity is inevitably sacrificed when using hydrogel electrolytes. The functional groups of the polymer matrix play a significant role in determining the transport of Zn^{2+}. Therefore, engineering the polymer matrix is a promising solution to this issue. Sulfobetaine monomers that contain sulfonate groups and quaternary ammonium groups, which carry negative and positive charges, respectively, are promising candidates for forming hydrogel with high ionic conductivity. The charged groups in the side chains of sulfobetaine zwitterionic hydrogels have moderate electrostatic interactions with electrolyte ions. They form the "ion migration channels" that facilitate the transfer of Zn^{2+} and anions, thus increasing the ionic conductivity [188]. Furthermore, the charged groups can firmly adhere to the

Zn anode surface, adjusting the electrode/electrolyte interface and avoiding their separation during battery operation (Fig. 8e) [187]. The strong electrostatic interaction between sulfobetaine and water also gives excellent water retention of gel electrolyte [189]. Nowadays, the development of polyzwitterionic hydrogel electrolyte is at the infant stage and there is much space for improvement. For example, more types of novel polyzwitterionic hydrogel containing both anionic groups (e.g., carboxylic, phosphate, and sulfate) and cationic groups (e.g., imidazolium), can be rationally designed and fabricated to improve the performance of hydrogel electrolytes.

The interfacial contact between electrode and electrolyte also plays a crucial role in the performance of batteries with hydrogels, which is different from liquid electrolytes that can readily wet the electrode surface. In contrast, gel electrolyte is usually polymerized outside the battery and then assembled with the electrodes to form RAZBs. They tend to form a poorly compatible quasi-solid-solid electrolyte/electrode interface, which can result in high interfacial impedance that impairs electrochemical performance. Therefore, it is essential to ensure the adhesion of the ex-situ synthesized hydrogel electrolyte to the Zn electrode. Otherwise, the prepared battery will suffer from severe dendrite formation and side reactions [190]. Even worse, the hydrogel electrolyte, which does not have good adhesion, tends to exfoliate from the electrodes, directly causing failure of RAZBs [191]. To circumvent this issue, high-adhesive hydrogel electrolytes have been developed recently. For instance, the cotton-derived cellulose/glycerin hydrogel adheres firmly to the Zn anode due to the abundant hydrogen bonding [192]. Besides, sodium lignosulfonate (SL)/PAM hydrogel

electrolyte brings a tightly integrated anode/electrolyte interface due to the strong interaction between sulfonate groups and Zn anode [193]. It is demonstrated that even after folding in half, the electrolyte does not fall off and there is almost no loss of capacity and no increase in impedance. In-situ polymerization is another promising approach to address the interfacial issues as demonstrated by Qin et al. [194]. The Zn anode-potassium persulfate (Zn-KPS) oxidation-reduction initiation system catalyzes the radical polymerization. This initiative results in strong interfacial bonding and good electrochemical performance through “chemical welding”, as well as significantly reduce the processing complexity of the hydrogel electrolytes. Furthermore, Li et al. [58] also used the in-situ polymerization method to synthesize PAM hydrogel at the surface of plasma-treated Zn foil. Gelation occurs after direct coating of the monomer solution on the anode surface. As a result, they obtained a layer of ultrathin and closely attached electrode-electrolyte integrated structure. The thin-film batteries are thereby easily implemented. This method provides a solution for the preparation of ultra-thin energy storage devices.

Noteworthily, Wu et al. [195] proposed an innovative method for fabricating hydrogel electrolytes. A chitosan foam framework was first prepared and then immersed into Zn^{2+}-saturated NaOH solution to coordinate the chitosan with Zn^{2+} (chitosan-Zn). Afterwards, the chitosan-Zn membrane was compressed to remove excess water and densify the membrane. The chitosan-Zn electrolyte was obtained by immersing the porous chitosan-Zn membrane in $ZnSO_4$ solution, followed by densification. It was shown that the mechanical strength of the densified chitosan-Zn^{2+}

complex was enhanced and aqueous electrolyte was confined in the nanoscale pores. This unique membrane design effectively prevents interfacial side reactions and dendrite penetration. More impressively, the as-developed quasi-solid electrolyte displays an ionic conductivity of as high as 72 mS cm^{-1}, which is close to that of aqueous electrolyte. As a result, the densified chitosan-Zn electrolyte enables the Zn anode to achieve a high CE of 99.7% and a long cycle life of >1000 cycles at a high current density of 50 mA cm^{-2}. Moreover, the chitosan-Zn electrolyte is non-flammable and fully biodegradable, offering great opportunities for developing green, eco-friendly, and sustainable RAZBs.

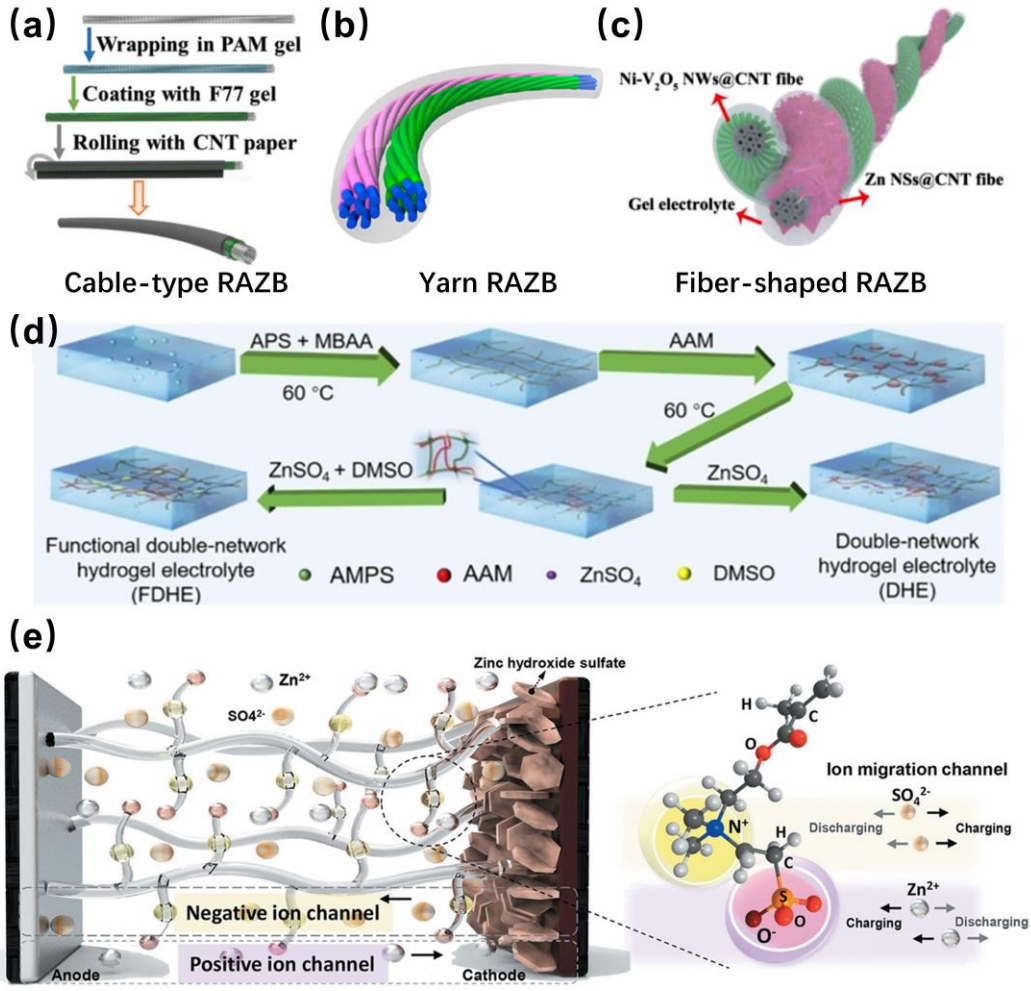

Fig. 8. (a) The cable-type battery. Reproduced with permission from [176]. Copyright 2019, Wiley-VCH. (b) The yarn battery. Reproduced with permission from [185]. Copyright 2018, American Chemical Society. (c) The fiber-shaped battery. Reproduced with permission from [186]. Copyright 2022, Elsevier. (d) The synthesis of PAMPS/PAAM dual-network hydrogel. Reproduced with permission from [71]. Copyright 2022, Elsevier. (e) Schematic of the sulfobetaine zwitterionic hydrogel electrolyte in a zinc-ion battery under an external electric field. Reproduced with permission from [187]. Copyright 2020, Elsevier.

3.3.1.2 Functionality of hydrogel electrolytes

More attractively, hydrogel electrolytes can be functionalized to cope with different scenarios, opening up great opportunities for developing advanced batteries that can be applied under abusive conditions. For example, when flexible energy storage devices (e.g., batteries and supercapacitors) are under large deformation, they may suffer from damage [196]. The ability to automatically repair the damage, or self-repairing, would be a promising solution to boost the service lifetime of these devices [197]. Hydrogel electrolytes that are rich in physical interactions offer great potential to realize this objective. As proof of concept, Niu's group [175] adopted an easy freezing/thawing strategy to prepare the PVA/$Zn(OTf)_2$ hydrogel electrolyte, which is a type of intrinsic self-healing material. The hydrogel can automatically repair itself after cutting without any external help, just by the hydrogen bonding between PVA molecular chains. More importantly, PVA/$Zn(OTf)_2$ hydrogel can still maintain excellent electrochemical performance after multiple cutting-self-repair processes. Likewise, physical dynamic crosslinking was adopted by Mai's group [198]. They prepared guar gum/borax hydrogel electrolytes with water-glycerol hybrid solvent. Glycerol was innovatively introduced to adsorb guar gum molecular chains through hydrogen bonding and thus limit its intramolecular rotation. Guar gum self-crimping is restricted and a large number of -OH are exposed. Under this circumstance, dynamic cross-linking between hydroxyl groups of guar gum and borax is constructed and the quasi-solid electrolyte acquires ultra-fast self-healing properties. It is worth mentioning that reversible covalent bonds, such as Diels-Alder reaction, borate ester bonds, and

disulfide bonds [199], can also be used to achieve self-healing properties, which hold potential for application in hydrogel-based RAZBs.

In addition to self-healing, the stimulus responsiveness of the hydrogel endows the batteries with unique features. For instance, the generation and accumulation of heat inside the batteries causes a continuous rise in temperature, which will accelerate HER and cause a surge in internal pressure. Fortunately, temperature-sensitive hydrogel electrolyte provides an option to alleviate this problem. For example, poly(*N*-isopropylacrylamide) (PNIPAM) has a temperature-dependent sol-gel transition behavior. Specifically, as the temperature increases, the hydrogen bonds between the solvent water molecules and the -NH- in side chain are gradually broken, reducing the solubility of the polymer in water (Fig. 9a). When reaching above the lower critical solution temperature (LCST), phase separation between the polymer and water occurs. Fascinated by this property, Mo et al. [200] synthesized a thermally sensitive PNIPAM-*co*-PAA hydrogel electrolyte. Experiments have confirmed that this material changes to a gel state, which is unfavorable to Zn^{2+} migration at high temperatures, causing a surge in the internal resistance of the battery and thus breaking in the circuit. RAZBs with self-protection capabilities exhibit greater safety and reliability when faced with thermal runaway. In addition, Qian's group [201] innovatively designed a thermoregulatory hydrogel electrolyte (TRHE) by integrating phase transition chains (i.e., PEG) with endothermic effect into agarose backbone for thermal management of RAZBs. When the internal temperature reaches the phase transition temperature, PEG can absorb the generated heat by changing to amorphous state (Fig. 9b). Therefore,

TRHE can cope with the thermal shock efficiently. More importantly, as shown in Fig. 9c and d, the TRHE confers RAZBs better rate performance in comparison to the blank electrolyte of 1 M $ZnSO_4$ and baseline hydrogel electrolyte without PEG. Even at 100 °C, the battery using TRHE can still cycle stably for a period.

Apart from high temperatures, the batteries should be able to operate under cold weather with temperatures below 0 °C, which requires the aqueous electrolyte not to freeze. One simple yet effective solution is to add organic solvents such as EG, glycerol, and DMSO into the hydrogel electrolytes. For example, in order to break the crystalline microregion of the PVA/borax hydrogel and thus lower the freezing point, Chen et al. [202] added a small amount of glycerol into the gel electrolyte. As a result, the -OH in glycerol formed hydrogen bonds with the -OH in PVA to weaken the interactions between macromolecular chains. Therefore, the difficulty of ice crystal formation inside the hydrogel network makes it possible for the electrolyte to work at low temperatures. Remarkably, even at a low temperature of -35 °C, the Zn//MnO_2 with the anti-freezing gel electrolyte can still deliver a high energy density of 25.8 mWh cm^{-3} and retain 53.3% of that value when the power density is increased to about 10-fold.

Additionally, the safety and stability of RAZBs make them potentially viable for biomedical use. However, the use of some toxic chemicals raises concerns when turning to practical applications, such as implantable devices. Using the electro-cross-linking method, Zhou's group [55] prepared a wire-shaped RAZB with Zn-alginate quasi-solid electrolyte (Fig. 9e). The superionic binds between the carboxylate group and Zn^{2+} were in situ formed without employing any chemical initiators and cross-linkers. This

strategy not only provides the battery with an excellent cycling stability, but also makes it highly biocompatible, which extends the applications of RAZBs.

These works have demonstrated the great promise of hydrogel for fabricating high-performance Zn batteries. Given the considerable tunability of polymers, e.g., materials (monomers, initiators, cross-linkers, fillers, solvents, etc.), polymerization methods, and processing and molding approaches, it can be anticipated that the design of multifunctional hydrogel electrolytes will continue to flourish. In future exploration, the hydrogel electrolyte should be reasonably designed based on the actual requirement of RAZBs, considering several factors including flexibility, mechanical properties, adhesion, self-healing properties, ionic conductivity, water retention, temperature adaptability, and environmental friendliness.

3.3.2 Inorganic salt hydrates electrolytes

In addition to polymer hydrogel electrolytes, Guo and coworkers [72] invented a novel inorganic quasi-solid electrolyte for RAZBs by directly mixing extremely high solid content of $CaSO_4 \cdot 2H_2O$ (CS) with a small amount of $ZnSO_4$ solution. Due to the unique interlayered structure and morphology, the liquid $ZnSO_4$ solution was absorbed on surface of the porous CS powders, which not only considerably reduces the amount of active water, thus suppressing side reactions, but also forms two continuous ion transportation networks of the quasi-solid electrolyte (Fig. 9f). More importantly, when applied in the batteries, the electrolyte can lead to in-situ formation of dual-phase SEI consisting of inner zinc hydroxysulfate layer and outer zinc hydroxysulfate/$CaSO_4 \cdot 2H_2O$ hybrid layer (Fig. 9g). The in-situ formed SEI can

dramatically improve the contact between electrode and electrolyte to reduce the interfacial resistance, isolate the direct contact of water with Zn to suppress the side reactions, and homogenize the electric field to regulate uniform Zn deposition. As a result, a Zn//Zn symmetric battery with this new quasi-solid electrolyte is able to achieve stable plating/stripping for over 3000 h, far outperforming that with conventional liquid electrolyte. When paired with a $Na_xV_2O_5{\cdot}nH_2O$ cathode, the full battery can maintain about 88% capacity after 50 normal cycles at 100 mA g^{-1}. Given the facile preparation and descent electrochemical performance of this novel quasi-solid electrolyte, this strategy represents a promising direction for developing high-performance quasi-solid electrolytes for RAZBs.

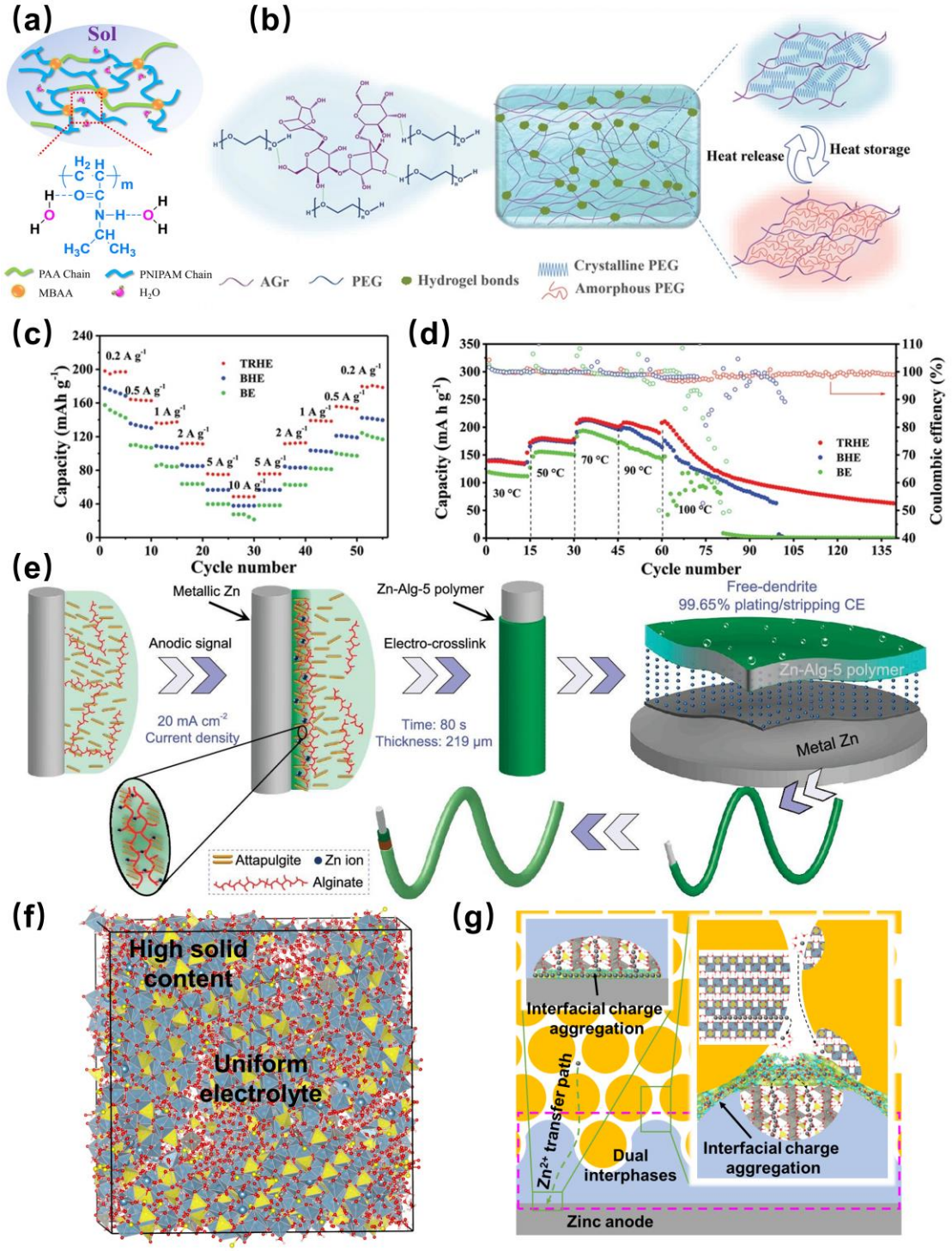

Fig. 9. (a) Mechanism of the reversible sol-gel transition at high temperature of PNIPAM-*co*-PAA hydrogel electrolyte. Reproduced with permission from [200]. Copyright 2018, Elsevier. (b) Composition and thermal regulation mechanism of the TRHE, (c) rate performance at room temperature, and (d) discharge capacity with

changed ambient temperature of Zn//$Na_xV_2O_5{\cdot}nH_2O$ batteries using different electrolytes. Reproduced with permission from [201]. Copyright 2022, Wiley-VCH. (e) Schematic of the in-situ preparation procedure of Zn-Alg-5 polymer electrolyte for a wire-shaped Zn battery. Reproduced with permission from [55]. Copyright 2023, Oxford University Press. (f) MD simulation of the quasi-solid electrolyte and (g) schematic diagram of Zn^{2+} migration path. Reproduced with permission from [72]. Copyright 2022, Wiley-VCH.

5 Conclusions and outlook

In summary, recent advances in electrolyte formulation for achieving stable and highly reversible Zn anodes are reviewed. The electrolyte engineering strategies are classified into different categories, including Zn salts (type and concentration), additives (salts, organics, and inorganic materials), and quasi-solid electrolytes. These strategies have been proven to be effective in addressing the dendrite and side reactions of Zn electrodes. Although considerable progress has been made via electrolyte engineering, which dramatically accelerates the development of RAZBs, several challenges still remain to be addressed.

First, the mechanisms of using electrolyte additives to improve the electrochemical performance remain unclear. Although several mechanistic models (e.g., electrostatic shielding, solvation structure) have been proposed, how the ions/species/charge are transported, as well as how the de-solvation and reaction process take place at the electrode/electrolyte interface, is illusive. For example, it has been widely reported that

partially replacing water in the solvation sheath of Zn^{2+} with additives can improve the reversibility of Zn plating/stripping. Nevertheless, what kind of solvation structure is beneficial to Zn deposition and dissolution and how the altered solvation structure impacts the electrochemical process remain unknown. Therefore, more fundamental studies are needed to establish an in-depth understanding of the electrolyte environment in the Zn electrochemistry. Theoretical studies (e.g., DFT, MD, phase-field modeling) coupled with advanced characterizations (e.g., Nuclear Magnetic Resonance (NMR) spectroscopy, Raman, AFM) appears to be a powerful approach to uncover the mechanisms of electrolyte engineering. In particular, in-situ techniques that can offer insights into the dynamic evolution of electrode/electrolyte interface/interphase are urgently needed.

Second, although the reported electrolyte engineering strategies have substantially suppressed dendrite and side reactions, these issues are not completely eliminated. It appears that single approach may not be able to enable Zn anodes to meet requirement for practical applications. One possible solution to further enhance the performance is combining two or more strategies. For instance, introducing additives in the hydrogel electrolyte or using both organic compounds and inorganic materials at the same time. These studies have already received attention and got promising preliminary achievements [203-206]. Moreover, electrolyte engineering can be coupled with interface or structural modification to achieve a synergistic effect in boosting the performance of RAZBs. For example, substrates can be modified to induce preferential Zn nucleation while additives can be added to further constrain the preferential Zn

growth and suppress side reactions. This two-pronged approach may address the challenges of Zn electrodes to a larger extent.

Third, even though the cycling life of Zn electrodes has been considerably extended via electrolyte engineering, most of the results are tested under relatively low current density or/and areal capacity. Moreover, thick Zn foils with a low utilization rate are typically used to evaluate the performance. These conditions deviate considerably from practical scenarios. Therefore, future works should take practical conditions, such as high areal capacity, high current density, and utilization of anode, into consideration to promote the commercialization of this technology. Additionally, current works mainly emphasize the effectiveness of electrolyte engineering in improving the performance of Zn electrolytes. However, we would like to point out that it is also of great significance to investigate the degradation/failure mechanisms of electrolyte engineering under more harsh conditions, which are essential for further development of robust electrolytes for practical RAZBs.

Finally, hydrogel electrolytes also show great promise for rechargeable Zn batteries due to their unique features, including being free of leakage, high flexibility, and great turnability. However, it remains challenging to simultaneously maintain high ionic conductivity, high mechanical strength, and superior electrode/electrolyte interface. Crosslinking polymers with desirable properties may be a promising solution. However, in addition to trial and error, high-throughput computing can be adopted to facilitate the screening of suitable polymers. Moreover, it is highly desired to establish a composition-structure-performance relationship that can guide the design of high-

performance quasi-solid electrolytes.

Aiming to solve the above existing problems and pave the way for transferring RAZBs from research laboratory to industry, the following viewpoints should be considered for future studies. First, normative, authoritative, and practice-oriented battery assembly and electrochemical measurement standards/protocols should be established and adopted so that the effectiveness of electrolyte strategies can be evaluated and compared under more unbiased and rigorous conditions. Moreover, it is foreseen that interdisciplinary collaboration will play an increasingly important role in the research of electrolytes for RAZBs. Emerging data-driven artificial intelligence techniques, such as machine learning, will revolutionize the research paradigm of RAZBs. As a complement to experiment and theoretical calculations, we believe its judicious combination with traditional approaches will significantly improve the efficiency of research and development of electrolyte engineering and RAZBs.

Declaration of Competing Interest

The authors declare no conflict of interest.

Acknowledgments

The work described in this paper was supported by the grants from the Research Grants Council of the Hong Kong Special Administrative Region, China (Project No. 16205721), Guangdong Basic and Applied Basic Research Foundation (Project No. 2021A1515011815), and PolyU Start-up Fund (Project No. 1-BDC4).

References

[1] A.M. Omer, Renew. Sust. Energ. Rev. 12 (9) (2008) 2265-2300.

[2] P. Poizot, F. Dolhem, Energy Environ. Sci. 4 (6) (2011) 2003-2019.

[3] F. Wang, J.D. Harindintwali, Z. Yuan, M. Wang, F. Wang, S. Li, Z. Yin, L. Huang, Y. Fu, L. Li, S.X. Chang, L. Zhang, J. Rinklebe, Z. Yuan, Q. Zhu, L. Xiang, D.C.W. Tsang, L. Xu, X. Jiang, J. Liu, N. Wei, M. Kastner, Y. Zou, Y.S. Ok, J. Shen, D. Peng, W. Zhang, D. Barcelo, Y. Zhou, Z. Bai, B. Li, B. Zhang, K. Wei, H. Cao, Z. Tan, L.B. Zhao, X. He, J. Zheng, N. Bolan, X. Liu, C. Huang, S. Dietmann, M. Luo, N. Sun, J. Gong, Y. Gong, F. Brahushi, T. Zhang, C. Xiao, X. Li, W. Chen, N. Jiao, J. Lehmann, Y.G. Zhu, H. Jin, A. Schaffer, J.M. Tiedje, J.M. Chen, Innovation 2 (4) (2021) 100180.

[4] M. Armand, J.M. Tarascon, Nature 451 (7179) (2008) 652-657.

[5] B. Dunn, H. Kamath, J.M. Tarascon, Science 334 (6058) (2011) 928-935.

[6] B. Obama, Science 355 (6321) (2017) 126-129.

[7] J.X. Hao, W.J. Wu, Q. Wang, D. Yan, G.H. Liu, S.L. Peng, J. Mater. Chem. A 8 (15) (2020) 7192-7196.

[8] N. Kittner, F. Lill, D.M. Kammen, Nat. Energy 2 (9) (2017) 1-6.

[9] Z.Y. Xu, M.H. Jing, J.G. Liu, C.W. Yan, X.Z. Fan, J. Mater. Sci. Technol. 136 (2023) 32-42.

[10] Z.Y. Xu, M.D. Zhu, K.Y. Zhang, X.H. Zhang, L.X. Xu, J.G. Liu, T. Liu, C.A.W. Yan, Energy Stor. Mater. 39 (2021) 166-175.

[11] T. Kim, W. Song, D.-Y. Son, L.K. Ono, Y. Qi, J. Mater. Chem. A 7 (7) (2019) 2942-2964.

[12] A. Yoshino, Angew. Chem. Int. Ed. 51 (24) (2012) 5798-5800.

[13] J. Kalhoff, G.G. Eshetu, D. Bresser, S. Passerini, ChemSusChem 8 (13) (2015) 2154-2175.

[14] J. Wen, Y. Yu, C. Chen, Mater. Express 2 (3) (2012) 197-212.

[15] J.B. Goodenough, Y. Kim, Chem. Mater. 22 (3) (2009) 587-603.

[16] C.A. Rufino Júnior, E. Riva Sanseverino, P. Gallo, D. Koch, Y. Kotak, H.-G. Schweiger, H. Zanin, J. Energy Chem. 78 (2023) 507-525.

[17] Y. Zhao, K.R. Adair, X. Sun, Energy Environ. Sci. 11 (10) (2018) 2673-2695.

[18] Y. Liu, C. Gao, L. Dai, Q. Deng, L. Wang, J. Luo, S. Liu, N. Hu, Small 16 (44) (2020) e2004096.

[19] J.Y. Hwang, S.T. Myung, Y.K. Sun, Chem. Soc. Rev. 46 (12) (2017) 3529-3614.

[20] N. Yabuuchi, K. Kubota, M. Dahbi, S. Komaba, Chem. Rev. 114 (23) (2014) 11636-11682.

[21] R. Rajagopalan, Y. Tang, X. Ji, C. Jia, H. Wang, Adv. Funct. Mater. 30 (12) (2020) 1909486.

[22] J.W. Choi, D. Aurbach, Nat. Rev. Mater. 1 (4) (2016) 1-16.

[23] Z.Y. Xu, W. Xiao, K.Y. Zhang, D.H. Zhang, H. Wei, X.H. Zhang, Z.Y. Zhang, N.W. Pu, J.G. Liu, C.W. Yan, J. Power Sources 450 (2020) 227686.

[24] Y. Li, J. Lu, ACS Energy Lett. 2 (6) (2017) 1370-1377.

[25] C. Xu, B. Li, H. Du, F. Kang, Angew. Chem. Int. Ed. 51 (4) (2012) 933-935.

[26] Z. Yi, G. Chen, F. Hou, L. Wang, J. Liang, Adv. Energy Mater. 11 (1) (2020) 2003065.
[27] D. Chao, W. Zhou, F. Xie, C. Ye, H. Li, M. Jaroniec, S.Z. Qiao, Sci. Adv. 6 (21) (2020) eaba4098.
[28] Z.Y. Xu, M.C. Wu, Batteries 8 (9) (2022) 117.
[29] C. Xie, Y. Li, Q. Wang, D. Sun, Y. Tang, H. Wang, Carbon Energy 2 (4) (2020) 540-560.
[30] D. Kundu, B.D. Adams, V. Duffort, S.H. Vajargah, L.F. Nazar, Nat. Energy 1 (10) (2016) 1-8.
[31] G. Fang, J. Zhou, A. Pan, S. Liang, ACS Energy Lett. 3 (10) (2018) 2480-2501.
[32] C.W. Mao, Y.X. Chang, X.T. Zhao, X.Y. Dong, Y.F. Geng, N. Zhang, L. Dai, X.W. Wu, L. Wang, Z.X. He, J. Energy Chem. 75 (2022) 135-153.
[33] P. Benjamin, The Voltaic Cell: Its Construction and Its Capacity, J. Wiley, 1893.
[34] T.P. Crompton, T.R. Crompton, Battery reference book, Newnes, 2000.
[35] K. Kordesch, Primary batteries—alkaline manganese dioxide-zinc batteries, in: Comprehensive Treatise of Electrochemistry, Springer, 1981, pp. 219-232.
[36] Y. Li, H. Dai, Chem. Soc. Rev. 43 (15) (2014) 5257-5275.
[37] U. Köhler, C. Antonius, P. Bäuerlein, J. Power Sources 127 (1-2) (2004) 45-52.
[38] F.R. Mclarnon, E.J. Cairns, J. Electrochem. Soc. 138 (2) (1991) 645-664.
[39] T. Yamamoto, T. Shoji, Inorg. Chim. Acta 117 (2) (1986) L27-L28.
[40] C.J. Xu, H.D. Du, B.H. Li, F.Y. Kang, Y.Q. Zeng, Electrochem Solid St 12 (4) (2009) A61-A65.
[41] H. Chen, J. Huang, S. Tian, L. Liu, T. Qin, L. Song, Y. Liu, Y. Zhang, X. Wu, S. Lei, S. Peng, Adv. Sci. 8 (14) (2021) e2004924.
[42] B. Yong, D. Ma, Y. Wang, H. Mi, C. He, P. Zhang, Adv. Energy Mater. 10 (45) (2020) 2002354.
[43] Z. Pan, X. Liu, J. Yang, X. Li, Z. Liu, X.J. Loh, J. Wang, Adv. Energy Mater. 11 (24) (2021) 2100608.
[44] W. Du, E.H. Ang, Y. Yang, Y. Zhang, M. Ye, C.C. Li, Energy Environ. Sci. 13 (10) (2020) 3330-3360.
[45] L.E. Blanc, D. Kundu, L.F. Nazar, Joule 4 (4) (2020) 771-799.
[46] Z. Kang, C. Wu, L. Dong, W. Liu, J. Mou, J. Zhang, Z. Chang, B. Jiang, G. Wang, F. Kang, C. Xu, ACS Sustain. Chem. Eng. 7 (3) (2019) 3364-3371.
[47] W. Guo, Z. Cong, Z. Guo, C. Chang, X. Liang, Y. Liu, W. Hu, X. Pu, Energy Stor. Mater. 30 (2020) 104-112.
[48] Q.P. Jian, Z.X. Guo, L.C. Zhang, M.C. Wu, T.S. Zhao, Chem. Eng. J. 425 (2021) 130643.
[49] Z. Cai, Y. Ou, J. Wang, R. Xiao, L. Fu, Z. Yuan, R. Zhan, Y. Sun, Energy Stor. Mater. 27 (2020) 205-211.
[50] G. Chen, Z. Sang, J. Cheng, S. Tan, Z. Yi, X. Zhang, W. Si, Y. Yin, J. Liang, F. Hou, Energy Stor. Mater. 50 (2022) 589-597.
[51] H. Yan, S. Li, Y. Nan, S. Yang, B. Li, Adv. Energy Mater. 11 (18) (2021) 2100186.
[52] Q. Jian, Y. Wan, Y. Lin, M. Ni, M. Wu, T. Zhao, ACS Appl. Mater. Interfaces 13

(2021) 52659-52669.
[53] Q. Jian, Y. Wan, J. Sun, M. Wu, T. Zhao, J. Mater. Chem. A 8 (38) (2020) 20175-20184.
[54] Y.Y. Li, H.L. Wong, J. Wang, W.L. Peng, Y.D. Shen, M.Y. Xu, Q. An, J.K. Kim, B. Yuan, W.A. Goddard, Z.T. Luo, Adv. Energy Mater. 12 (2022) 2202983.
[55] X. Xie, J. Li, Z. Xing, B. Lu, S. Liang, J. Zhou, Natl. Sci. Rev. 10 (3) (2023) nwac281.
[56] B. Luo, Y. Wang, L. Sun, S. Zheng, G. Duan, Z. Bao, Z. Ye, J. Huang, J. Energy Chem. 77 (2023) 632-641.
[57] H. Fu, Q. Wen, P.Y. Li, Z.Y. Wang, Z.J. He, C. Yan, J. Mao, K.H. Dai, X.H. Zhang, J.C. Zheng, J. Energy Chem. 73 (2022) 387-393.
[58] J. Li, P. Yang, X. Li, C. Jiang, J. Yun, W. Yan, K. Liu, H.J. Fan, S.W. Lee, ACS Energy Lett. 8 (2022) 1-8.
[59] T.T. Wang, P.J. Wang, L. Pan, Z.X. He, L. Dai, L. Wang, S.D. Liu, S.C. Jun, B.A. Lu, S.Q. Liang, J. Zhou, Adv. Energy Mater. 13 (5) (2023) 2203523.
[60] Q. Liu, Z. Yu, R. Zhou, B. Zhang, Adv. Funct. Mater. 33 (5) (2022) 2210290.
[61] Q. Liu, Y. Wang, X. Hong, R. Zhou, Z. Hou, B. Zhang, Adv. Energy Mater. 12 (20) (2022) 2200318.
[62] W. Hu, J. Ju, Y. Zhang, W. Tan, N. Deng, W. Liu, W. Kang, B. Cheng, J. Mater. Chem. A 10 (46) (2022) 24761-24771.
[63] Y. An, Y. Tian, Q. Man, H. Shen, C. Liu, Y. Qian, S. Xiong, J. Feng, Y. Qian, ACS Nano 16 (4) (2022) 6755-6770.
[64] Y. Song, P. Ruan, C. Mao, Y. Chang, L. Wang, L. Dai, P. Zhou, B. Lu, J. Zhou, Z. He, Nanomicro Lett 14 (1) (2022) 218.
[65] Y.F. Liu, S.D. Liu, X.S. Xie, Z.C. Li, P.J. Wang, B.A. Lu, S.Q. Liang, Y. Tang, J. Zhou, Infomat (2022) e12374.
[66] Y. Li, P. Wu, W. Zhong, C. Xie, Y. Xie, Q. Zhang, D. Sun, Y. Tang, H. Wang, Energy Environ. Sci. 14 (10) (2021) 5563-5571.
[67] D.L. Han, Z.X. Wang, H.T. Lu, H. Li, C.J. Cui, Z.C. Zhang, R. Sun, C.N. Geng, Q.H. Liang, X.X. Guo, Y.B. Mo, X. Zhi, F.Y. Kang, Z. Weng, Q.H. Yang, Adv. Energy Mater. 12 (9) (2022) 2102982.
[68] M. Qiu, P. Sun, Y. Wang, L. Ma, C. Zhi, W. Mai, Angew. Chem. Int. Ed. (2022).
[69] W. Zhang, Q. Zhao, Y. Hou, Z. Shen, L. Fan, S. Zhou, Y. Lu, L.A. Archer, Sci. Adv. 7 (49) (2021) eabl3752.
[70] W. Zhang, M. Dong, K. Jiang, D. Yang, X. Tan, S. Zhai, R. Feng, N. Chen, G. King, H. Zhang, H. Zeng, H. Li, M. Antonietti, Z. Li, Nature Communications 13 (1) (2022) 5348.
[71] Y. Liu, H. He, A. Gao, J. Ling, F. Yi, J. Hao, Q. Li, D. Shu, Chem. Eng. J. 446 (2022) 137021.
[72] S. Guo, L.P. Qin, C. Hu, L.Y. Li, Z.G. Luo, G.Z. Fang, S.Q. Liang, Adv. Energy Mater. 12 (25) (2022) 2200730.
[73] C. Zhang, J. Holoubek, X. Wu, A. Daniyar, L. Zhu, C. Chen, D.P. Leonard, I.A. Rodriguez-Perez, J.X. Jiang, C. Fang, X. Ji, ChemComm 54 (100) (2018) 14097-14099.

[74] K. Wu, F. Ning, J. Yi, X. Liu, J. Qin, Y. Liu, J. Zhang, J. Energy Chem. 69 (2022) 237-243.
[75] E. Budevski, G. Staikov, W.J. Lorenz, Electrochim. Acta 45 (15-16) (2000) 2559-2574.
[76] D.H. Wang, Q. Li, Y.W. Zhao, H. Hong, H.F. Li, Z.D. Huang, G.J. Liang, Q. Yang, C.Y. Zhi, Adv. Energy Mater. 12 (9) (2022) 2102707.
[77] Q. Yang, Q. Li, Z. Liu, D. Wang, Y. Guo, X. Li, Y. Tang, H. Li, B. Dong, C. Zhi, Adv. Mater. 32 (48) (2020) e2001854.
[78] Q. Yang, G. Liang, Y. Guo, Z. Liu, B. Yan, D. Wang, Z. Huang, X. Li, J. Fan, C. Zhi, Adv. Mater. 31 (43) (2019) e1903778.
[79] W. Lu, C. Xie, H. Zhang, X. Li, ChemSusChem 11 (23) (2018) 3996-4006.
[80] D. Xie, Z.W. Wang, Z.Y. Gu, W.Y. Diao, F.Y. Tao, C. Liu, H.Z. Sun, X.L. Wu, J.W. Wang, J.P. Zhang, Adv. Funct. Mater. 32 (32) (2022) 2204066.
[81] F. Ding, W. Xu, G.L. Graff, J. Zhang, M.L. Sushko, X. Chen, Y. Shao, M.H. Engelhard, Z. Nie, J. Xiao, X. Liu, P.V. Sushko, J. Liu, J.G. Zhang, J. Am. Chem. Soc. 135 (11) (2013) 4450-4456.
[82] J. Zheng, J. Yin, D. Zhang, G. Li, D.C. Bock, T. Tang, Q. Zhao, X. Liu, A. Warren, Y. Deng, S. Jin, A.C. Marschilok, E.S. Takeuchi, K.J. Takeuchi, C.D. Rahn, L.A. Archer, Sci. Adv. 6 (25) (2020) eabb1122.
[83] G. Garcia, E. Ventosa, W. Schuhmann, ACS Appl. Mater. Interfaces 9 (22) (2017) 18691-18698.
[84] Q. Li, Y. Wang, F. Mo, D. Wang, G. Liang, Y. Zhao, Q. Yang, Z. Huang, C. Zhi, Adv. Energy Mater. 11 (14) (2021) 2003931.
[85] A. Bayaguud, Y. Fu, C. Zhu, J. Energy Chem. 64 (2022) 246-262.
[86] H. Liu, Q. Zhou, Q. Xia, Y. Lei, X. Long Huang, M. Tebyetekerwa, X. Song Zhao, J. Energy Chem. 77 (2023) 642-659.
[87] L. Wang, Y. Zhang, H. Hu, H.Y. Shi, Y. Song, D. Guo, X.X. Liu, X. Sun, ACS Appl. Mater. Interfaces 11 (45) (2019) 42000-42005.
[88] W. Xin, L. Miao, L. Zhang, H. Peng, Z. Yan, Z. Zhu, ACS Materials Letters 3 (12) (2021) 1819-1825.
[89] D. Li, L. Cao, T. Deng, S. Liu, C. Wang, Angew. Chem. Int. Ed. 60 (23) (2021) 13035-13041.
[90] Z. Tao, Y. Zhu, Z. Zhou, A. Wang, Y. Tan, Z. Chen, M. Yu, Y. Yang, Small 18 (22) (2022) e2107971.
[91] W. Yang, X. Du, J. Zhao, Z. Chen, J. Li, J. Xie, Y. Zhang, Z. Cui, Q. Kong, Z. Zhao, C. Wang, Q. Zhang, G. Cui, Joule 4 (7) (2020) 1557-1574.
[92] C. Li, X. Xie, S. Liang, J. Zhou, Energy Environ. Mater. 3 (2) (2020) 146-159.
[93] J. Fu, Z.P. Cano, M.G. Park, A. Yu, M. Fowler, Z. Chen, Adv. Mater. 29 (7) (2017) 1604685.
[94] L. Ma, S. Chen, H. Li, Z. Ruan, Z. Tang, Z. Liu, Z. Wang, Y. Huang, Z. Pei, J.A. Zapien, C. Zhi, Energy Environ. Sci. 11 (9) (2018) 2521-2530.
[95] N. Zhang, F. Cheng, Y. Liu, Q. Zhao, K. Lei, C. Chen, X. Liu, J. Chen, J. Am. Chem. Soc. 138 (39) (2016) 12894-12901.
[96] S. Huang, J. Zhu, J. Tian, Z. Niu, Chem. Eur. J. 25 (64) (2019) 14480-14494.

[97] G.L. Li, Z. Yang, Y. Jiang, C.H. Jin, W. Huang, X.L. Ding, Y.H. Huang, Nano Energy 25 (2016) 211-217.
[98] S. Kim, J. Lee, S. Kim, S. Kim, J. Yoon, Energy Technol. 6 (2) (2018) 340-344.
[99] X. Xu, M. Song, M. Li, Y. Xu, L. Sun, L. Shi, Y. Su, C. Lai, C. Wang, Chem. Eng. J. 454 (2023) 140364.
[100] X. Xu, H. Su, J.T. Zhang, Y. Zhong, Y.F. Xu, Z. Qiu, H.B. Wu, X.L. Wang, C.D. Gu, J.P. Tu, ACS Energy Lett. 7 (2022) 4459-4468.
[101] M. Xu, T. Zhu, J.Z.H. Zhang, J. Phys. Chem. A 123 (30) (2019) 6587-6595.
[102] O. Borodin, J. Self, K.A. Persson, C.S. Wang, K. Xu, Joule 4 (1) (2020) 69-100.
[103] S. Wu, Y. Chen, T. Jiao, J. Zhou, J. Cheng, B. Liu, S. Yang, K. Zhang, W. Zhang, Adv. Energy Mater. 9 (47) (2019) 1902915.
[104] Q. Zhang, Y. Ma, Y. Lu, X. Zhou, L. Lin, L. Li, Z. Yan, Q. Zhao, K. Zhang, J. Chen, Angew. Chem. Int. Ed. 60 (43) (2021) 23357-23364.
[105] L. Suo, O. Borodin, T. Gao, M. Olguin, J. Ho, X. Fan, C. Luo, C. Wang, K. Xu, Science 350 (6263) (2015) 938-943.
[106] P. Samanta, S. Ghosh, A. Kundu, P. Samanta, N. Chandra Murmu, T. Kuila, J. Energy Chem. 78 (2023) 350-373.
[107] F. Wang, O. Borodin, T. Gao, X. Fan, W. Sun, F. Han, A. Faraone, J.A. Dura, K. Xu, C. Wang, Nat. Mater. 17 (6) (2018) 543-549.
[108] L. Zhang, I.A. Rodriguez-Perez, H. Jiang, C. Zhang, D.P. Leonard, Q.B. Guo, W.F. Wang, S.M. Han, L.M. Wang, X.L. Ji, Adv. Funct. Mater. 29 (30) (2019) 1902653.
[109] Y. Zhu, J. Yin, X. Zheng, A.-H. Emwas, Y. Lei, O.F. Mohammed, Y. Cui, H.N. Alshareef, Energy Environ. Sci. 14 (8) (2021) 4463-4473.
[110] L. Qian, H. Zhu, T. Qin, R. Yao, J. Zhao, F. Kang, C. Yang, Adv. Funct. Mater. (2023) 2301118.
[111] S.G. Bratsch, J. Phys. Chem. Ref. Data 18 (1) (1989) 1-21.
[112] F. Mansfeld, S. Gilman, J. Electrochem. Soc. 117 (5) (1970) 588-592.
[113] G. Chang, S.J. Liu, Y.N. Fu, X. Hao, W. Jin, X.B. Ji, J.G. Hu, Adv. Mater. Interfaces 6 (23) (2019) 1901358.
[114] J.M. Wang, L. Zhang, C. Zhang, J.Q. Zhang, J. Power Sources 102 (1-2) (2001) 139-143.
[115] Y. Xu, J. Zhu, J. Feng, Y. Wang, X. Wu, P. Ma, X. Zhang, G. Wang, X. Yan, Energy Stor. Mater. 38 (2021) 299-308.
[116] X. Zhou, K. Ma, Q. Zhang, G. Yang, C. Wang, Nano Res. 15 (9) (2022) 8039-8047.
[117] N. Li, G. Li, C. Li, H. Yang, G. Qin, X. Sun, F. Li, H.M. Cheng, ACS Appl. Mater. Interfaces 12 (12) (2020) 13790-13796.
[118] B.W. Olbasa, F.W. Fenta, S.F. Chiu, M.C. Tsai, C.J. Huang, B.A. Jote, T.T. Beyene, Y.F. Liao, C.H. Wang, W.N. Su, H. Dai, B.J. Hwang, ACS Appl. Energy Mater. 3 (5) (2020) 4499-4508.
[119] Q. Zhang, Y. Ma, Y. Lu, Y. Ni, L. Lin, Z. Hao, Z. Yan, Q. Zhao, J. Chen, J. Am. Chem. Soc. 144 (40) (2022) 18435-18443.
[120] R. Zhao, H. Wang, H. Du, Y. Yang, Z. Gao, L. Qie, Y. Huang, Nature

Communications 13 (1) (2022) 3252.
[121] X. Guo, Z. Zhang, J. Li, N. Luo, G.-L. Chai, T.S. Miller, F. Lai, P. Shearing, D.J.L. Brett, D. Han, Z. Weng, G. He, I.P. Parkin, ACS Energy Lett. 6 (2) (2021) 395-403.
[122] J. Wang, Y. Yang, Y. Wang, S. Dong, L. Cheng, Y. Li, Z. Wang, L. Trabzon, H. Wang, ACS Nano 16 (10) (2022) 15770-15778.
[123] Y. Shang, P. Kumar, T. Musso, U. Mittal, Q. Du, X. Liang, D. Kundu, Adv. Funct. Mater. 32 (26) (2022) 2200606.
[124] Q. Ma, R. Gao, Y. Liu, H. Dou, Y. Zheng, T. Or, L. Yang, Q. Li, Q. Cu, R. Feng, Z. Zhang, Y. Nie, B. Ren, D. Luo, X. Wang, A. Yu, Z. Chen, Adv. Mater. 34 (49) (2022) e2207344.
[125] J. Hao, L. Yuan, C. Ye, D. Chao, K. Davey, Z. Guo, S.Z. Qiao, Angew. Chem. Int. Ed. 60 (13) (2021) 7366-7375.
[126] N. Wang, Y. Yang, X. Qiu, X. Dong, Y. Wang, Y. Xia, ChemSusChem 13 (20) (2020) 5556-5564.
[127] J.Y. Duan, L.F. Min, T. Yang, M.M. Chen, C.Y. Wang, J. Alloys Compd. 918 (2022) 165619.
[128] Y. Zhang, M. Zhu, K. Wu, F. Yu, G. Wang, G. Xu, M. Wu, H.-K. Liu, S.-X. Dou, C. Wu, J. Mater. Chem. A 9 (7) (2021) 4253-4261.
[129] R.Z. Qin, Y.T. Wang, M.Z. Zhang, Y. Wang, S.X. Ding, A.Y. Song, H.C. Yi, L.Y. Yang, Y.L. Song, Y.H. Cui, J. Liu, Z.Q. Wang, S.N. Li, Q.H. Zhao, F. Pan, Nano Energy 80 (2021) 105478.
[130] G. Ma, L. Miao, Y. Dong, W. Yuan, X. Nie, S. Di, Y. Wang, L. Wang, N. Zhang, Energy Stor. Mater. 47 (2022) 203-210.
[131] L.C. Miao, R.H. Wang, W.L. Xin, L. Zhang, Y.H. Geng, H.L. Peng, Z.C. Yan, D.T. Jiang, Z.F. Qian, Z.Q. Zhu, Energy Stor. Mater. 49 (2022) 445-453.
[132] H. Du, K. Wang, T. Sun, J. Shi, X. Zhou, W. Cai, Z. Tao, Chem. Eng. J. 427 (2022) 131705.
[133] L. Miao, R. Wang, S. Di, Z. Qian, L. Zhang, W. Xin, M. Liu, Z. Zhu, S. Chu, Y. Du, N. Zhang, ACS Nano 16 (6) (2022) 9667-9678.
[134] H.J. Huang, D.M. Xie, J.C. Zhao, P.H. Rao, W.M. Choi, K. Davey, J.F. Mao, Adv. Energy Mater. 12 (38) (2022) 2202419.
[135] B. Qiu, L.Z. Xie, G.Q. Zhang, K.J. Cheng, Z.W. Lin, W. Liu, C.X. He, P.X. Zhang, H.W. Mi, Chem. Eng. J. 449 (2022) 137843.
[136] Y. Dong, L. Miao, G. Ma, S. Di, Y. Wang, L. Wang, J. Xu, N. Zhang, Chem. Sci. 12 (16) (2021) 5843-5852.
[137] W.K. Wang, C. Yang, X.W. Chi, J.H. Liu, B. Wen, Y. Liu, Energy Stor. Mater. 53 (2022) 774-782.
[138] J. Xiang, M. Luo, X. Wu, Y. Zhu, X. Zhang, H. Pan, W. Sun, M. Yan, Y. Lu, Y. Jiang, ChemComm 58 (65) (2022) 9104-9107.
[139] L.J. Zhou, F.X. Wang, F. Yang, X.Q. Liu, Y.X. Yu, D.Z. Zheng, X.H. Lu, Angew. Chem. Int. Ed. 61 (40) (2022) e202208051.
[140] W. Deng, Z. Xu, X. Wang, Energy Stor. Mater. 52 (2022) 52-60.
[141] L. Cao, D. Li, E. Hu, J. Xu, T. Deng, L. Ma, Y. Wang, X.Q. Yang, C. Wang, J.

Am. Chem. Soc. 142 (51) (2020) 21404-21409.
[142] Z. Hou, H. Tan, Y. Gao, M.H. Li, Z.H. Lu, B. Zhang, J. Mater. Chem. A 8 (37) (2020) 19367-19374.
[143] H.A. Zhao, Q. Fu, X.L. Luo, S. Indris, M. Bauer, Y.Z. Wang, H. Ehrenberg, M. Knapp, Y.J. Wei, Energy Stor. Mater. 50 (2022) 464-472.
[144] C. Meng, W.D. He, Z. Kong, Z.Y. Liang, H.P. Zhao, Y. Lei, Y.Z. Wu, X.P. Hao, Chem. Eng. J. 450 (2022) 138265.
[145] D. Feng, F. Cao, L. Hou, T. Li, Y. Jiao, P. Wu, Small 17 (42) (2021) e2103195.
[146] Z. Zhao, J. Yin, J. Yin, X. Guo, Y. Lei, Z. Tian, Y. Zhu, O.F. Mohammed, H.N. Alshareef, Energy Stor. Mater. 55 (2023) 479-489.
[147] Q.P. Jian, T.S. Wang, J. Sun, M.C. Wu, T.S. Zhao, Energy Stor. Mater. 53 (2022) 559-568.
[148] S.J. Zhang, J. Hao, Y. Zhu, H. Li, Z. Lin, S.Z. Qiao, Angew. Chem. Int. Ed. (2023) https://doi.org/10.1002/anie.202301570.
[149] C. Huang, X. Zhao, Y.S. Hao, Y.J. Yang, Y. Qian, G. Chang, Y. Zhang, Q.L. Tang, A.P. Hu, X.H. Chen, Energy Environ. Sci. (2023) https://doi.org/10.1039/d1033ee00045a.
[150] J. Cao, D. Zhang, R. Chanajaree, Y. Yue, Z. Zeng, X. Zhang, J. Qin, Adv. Powder Mater. 1 (1) (2022) 100007.
[151] M.H. Luo, C.Y. Wang, H.T. Lu, Y.H. Lu, B.B. Xu, W.P. Sun, H.G. Pan, M. Yan, Y.Z. Jiang, Energy Stor. Mater. 41 (2021) 515-521.
[152] Y.F. Cao, X.H. Tang, L.G. Li, H.F. Tu, Y.Z. Hu, Y.Y. Yu, S. Cheng, H.Z. Lin, L.W. Zhang, J.T. Di, Y.Y. Zhang, M.N. Liu, Nano Res. (2022) https://doi.org/10.1007/s12274-12022-14726-12273.
[153] M.J. Qiu, P. Sun, A.M. Qin, G.F. Cui, W.J. Mai, Energy Stor. Mater. 49 (2022) 463-470.
[154] H.Y. Qin, W. Kuang, N. Hu, X.M. Zhong, D. Huang, F. Shen, Z.W. Wei, Y.P. Huang, J. Xu, H.B. He, Adv. Funct. Mater. 32 (47) (2022) 2206695.
[155] M.J. Rosen, J.T. Kunjappu, Surfactants and interfacial phenomena, John Wiley & Sons, 2012.
[156] M. Wang, X. Wu, D. Yang, H. Zhao, L. He, J. Su, X. Zhang, X. Yin, K. Zhao, Y. Wang, Y. Wei, Chem. Eng. J. 451 (2023) 138589.
[157] A. Bayaguud, X. Luo, Y.P. Fu, C.B. Zhu, ACS Energy Lett. 5 (9) (2020) 3012-3020.
[158] K.E. Sun, T.K. Hoang, T.N. Doan, Y. Yu, X. Zhu, Y. Tian, P. Chen, ACS Appl. Mater. Interfaces 9 (11) (2017) 9681-9687.
[159] Z.G. Hou, X.Q. Zhang, X.N. Li, Y.C. Zhu, J.W. Liang, Y.T. Qian, J. Mater. Chem. A 5 (2) (2017) 730-738.
[160] J.N. Hao, J. Long, B. Li, X.L. Li, S.L. Zhang, F.H. Yang, X.H. Zeng, Z.H. Yang, W.K. Pang, Z.P. Guo, Adv. Funct. Mater. 29 (34) (2019) 1903605.
[161] Y.X. Lin, Z.X. Mai, H.K. Liang, Y. Li, G.Z. Yang, C.X. Wang, Energy Environ. Sci. 16 (2) (2023) 687-697.
[162] S.J. Banik, R. Akolkar, J. Electrochem. Soc. 160 (11) (2013) D519-D523.
[163] Y. Jin, K.S. Han, Y.Y. Shao, M.L. Sushko, J. Xiao, H.L. Pan, J. Liu, Adv. Funct.

Mater. 30 (43) (2020) 2003932.
[164] S. Jin, D. Zhang, A. Sharma, Q. Zhao, Y. Shao, P. Chen, J. Zheng, J. Yin, Y. Deng, P. Biswal, L.A. Archer, Small 17 (33) (2021) e2101798.
[165] S. Jin, J. Yin, X. Gao, A. Sharma, P. Chen, S. Hong, Q. Zhao, J. Zheng, Y. Deng, Y.L. Joo, L.A. Archer, Nature Communications 13 (1) (2022) 2283.
[166] Q. Zhang, J. Luan, L. Fu, S. Wu, Y. Tang, X. Ji, H. Wang, Angew. Chem. Int. Ed. 58 (44) (2019) 15841-15847.
[167] C.X. Lin, Y.C. Liu, X.X. Zhang, X.F. Miao, Y.Q. Chen, S.J. Chen, Y.N. Zhang, J. Power Sources 549 (2022) 232078.
[168] Q. Meng, R.Y. Zhao, P.H. Cao, Q.X. Bai, J.J. Tang, G.D. Liu, X.Y. Zhou, J. Yang, Chem. Eng. J. 447 (2022) 137471.
[169] J. Xu, W. Lv, W. Yang, Y. Jin, Q. Jin, B. Sun, Z. Zhang, T. Wang, L. Zheng, X. Shi, B. Sun, G. Wang, ACS Nano 16 (7) (2022) 11392-11404.
[170] H. Dong, X. Hu, G. He, Nanoscale 14 (39) (2022) 14544-14551.
[171] C. Sun, C. Wu, X. Gu, C. Wang, Q. Wang, Nanomicro Lett 13 (1) (2021) 89.
[172] J. Abdulla, J. Cao, D. Zhang, X. Zhang, C. Sriprachuabwong, S. Kheawhom, P. Wangyao, J. Qin, ACS Appl. Energy Mater. 4 (5) (2021) 4602-4609.
[173] J. Gao, X. Xie, S. Liang, B. Lu, J. Zhou, Nanomicro Lett 13 (1) (2021) 69.
[174] Y. Pan, Z. Liu, S. Liu, L. Qin, Y. Yang, M. Zhou, Y. Sun, X. Cao, S. Liang, G. Fang, Adv. Energy Mater. 13 (11) (2023) 2203766.
[175] S. Huang, F. Wan, S.S. Bi, J.C. Zhu, Z.Q. Niu, J. Chen, Angew. Chem. Int. Ed. 58 (13) (2019) 4313-4317.
[176] L.T. Ma, S.M. Chen, C.B. Long, X.L. Li, Y.W. Zhao, Z.X. Liu, Z.D. Huang, B.B. Dong, J.A. Zapien, C.Y. Zhi, Adv. Energy Mater. 9 (45) (2019) 1902446.
[177] S. Zhang, N. Yu, S. Zeng, S. Zhou, M. Chen, J. Di, Q. Li, J. Mater. Chem. A 6 (26) (2018) 12237-12243.
[178] J. Liu, M. Hu, J. Wang, N. Nie, Y. Wang, Y. Wang, J. Zhang, Y. Huang, Nano Energy 58 (2019) 338-346.
[179] D. Wang, H. Li, Z. Liu, Z. Tang, G. Liang, F. Mo, Q. Yang, L. Ma, C. Zhi, Small 14 (51) (2018) e1803978.
[180] Q. Li, X. Cui, Q. Pan, ACS Appl. Mater. Interfaces 11 (42) (2019) 38762-38770.
[181] Z.X. Liu, D.H. Wang, Z.J. Tang, G.J. Liang, Q. Yang, H.F. Li, L.T. Ma, F.N. Mo, C.Y. Zhi, Energy Stor. Mater. 23 (2019) 636-645.
[182] C. Liu, W. Xu, C. Mei, M. Li, W. Chen, S. Hong, W.Y. Kim, S.y. Lee, Q. Wu, Adv. Energy Mater. 11 (25) (2021) 2003902.
[183] H.F. Li, Q. Yang, F.N. Mo, G.J. Liang, Z.X. Liu, Z.J. Tang, L.T. Ma, J. Liu, Z.C. Shi, C.Y. Zhi, Energy Stor. Mater. 19 (2019) 94-101.
[184] C. Yan, Y. Wang, X. Deng, Y. Xu, Nanomicro Lett 14 (1) (2022) 98.
[185] H. Li, Z. Liu, G. Liang, Y. Huang, Y. Huang, M. Zhu, Z. Pei, Q. Xue, Z. Tang, Y. Wang, B. Li, C. Zhi, ACS Nano 12 (4) (2018) 3140-3148.
[186] T. Li, Q. Xu, M. Waqar, H. Yang, W. Gong, J. Yang, J. Zhong, Z. Liu, Energy Stor. Mater. 55 (2023) 64-72.
[187] F.N. Mo, Z. Chen, G.J. Liang, D.H. Wang, Y.W. Zhao, H.F. Li, B.B. Dong, C.Y. Zhi, Adv. Energy Mater. 10 (16) (2020) 2000035.

[188] W.T. Zhang, F.J. Guo, H.Y. Mi, Z.S. Wu, C.C. Ji, C.C. Yang, J.S. Qiu, Adv. Energy Mater. 12 (40) (2022) 2202219.
[189] K.T. Leng, G.J. Li, J.J. Guo, X.Y. Zhang, A.X. Wang, X.J. Liu, J.Y. Luo, Adv. Funct. Mater. 30 (23) (2020) 2001317.
[190] R. Ma, Z. Xu, X. Wang, Energy Environ. Mater. (2023) e12464.
[191] J. Duan, W. Xie, P. Yang, J. Li, G. Xue, Q. Chen, B. Yu, R. Liu, J. Zhou, Nano Energy 48 (2018) 569-574.
[192] M. Chen, J. Chen, W. Zhou, X. Han, Y. Yao, C.P. Wong, Adv. Mater. 33 (9) (2021) e2007559.
[193] J. Li, P. Yu, S. Zhang, Z. Wen, Y. Wen, W. Zhou, X. Dong, Y. Liu, Y. Liang, J. Colloid Interface Sci. 600 (2021) 586-593.
[194] Y. Qin, H. Li, C. Han, F. Mo, X. Wang, Adv. Mater. 34 (44) (2022) e2207118.
[195] M.L. Wu, Y. Zhang, L. Xu, C.P. Yang, M. Hong, M.J. Cui, B.C. Clifford, S.M. He, S.S. Jing, Y. Yao, L.B. Hu, Matter 5 (10) (2022) 3402-3416.
[196] Q. Liu, X. Hong, X. You, X. Zhang, X. Zhao, X. Chen, M. Ye, X. Liu, Energy Stor. Mater. 24 (2020) 541-549.
[197] T.F. Qin, S.L. Peng, J.X. Hao, Y.X. Wen, Z.L. Wang, X.F. Wang, D.Y. He, J.C. Zhang, J. Hou, G.Z. Cao, Adv. Energy Mater. 7 (20) (2017) 1700409.
[198] Q. Liu, R.P. Chen, L. Xu, Y. Liu, Y.H. Dai, M. Huang, L.Q. Mai, ACS Energy Lett. 7 (8) (2022) 2825-2832.
[199] M.M. Perera, N. Ayres, Polym Chem-Uk 11 (8) (2020) 1410-1423.
[200] F. Mo, H. Li, Z. Pei, G. Liang, L. Ma, Q. Yang, D. Wang, Y. Huang, C. Zhi, Sci. Bull. 63 (16) (2018) 1077-1086.
[201] Y. Meng, L.F. Zhang, M.J. Peng, D.N. Shen, C.H. Zhu, S.Y. Qian, J. Liu, Y.F. Cao, C.L. Yan, J.Q. Zhou, T. Qian, Adv. Funct. Mater. 32 (46) (2022) 2206653.
[202] M. Chen, W. Zhou, A. Wang, A. Huang, J. Chen, J. Xu, C.-P. Wong, J. Mater. Chem. A 8 (14) (2020) 6828-6841.
[203] C. Li, R. Kingsbury, L. Zhou, A. Shyamsunder, K.A. Persson, L.F. Nazar, ACS Energy Lett. 7 (1) (2022) 533-540.
[204] Y. Zhang, D. Wu, F. Huang, Y. Cai, Y. Li, H. Ke, P. Lv, Q. Wei, Adv. Funct. Mater. 32 (34) (2022) 2203204.
[205] S. Chen, P. Sun, J. Humphreys, P. Zou, M. Zhang, G. Jeerh, S. Tao, Energy Stor. Mater. 42 (2021) 240-251.
[206] C. Li, X. Xie, H. Liu, P. Wang, C. Deng, B. Lu, J. Zhou, S. Liang, Natl. Sci. Rev. 9 (3) (2022) nwab177.